

# Searches for New Phenomena at the Tevatron and at HERA

Arnd Meyer

III. Phys. Inst. A, RWTH Aachen, 52074 Aachen, Germany

E-mail: meyera@physik.rwth-aachen.de

Recent results on searches for new physics at Run II of the Tevatron and highlights from HERA are reported. The searches cover many different final states and a wide range of models. All analyses have at this point led to negative results, but some interesting anomalies have been found.

## 1. Introduction

For all of the deficits of the standard model (SM) that we know about since many years – be it the non-unification of couplings at a high scale, the quadratic divergences in the loop corrections to the Higgs boson mass, or the lack of a decent dark matter candidate – a large number of solutions has been proposed. We know that within the standard model, the  $W_L W_L$  scattering amplitude violates the unitarity bound at a center of mass energy  $\simeq 1.7$  TeV [1], and one solution to this problem is offered by the Higgs mechanism [2], through the introduction of a massive scalar particle. To successfully address the  $W_L W_L$  scattering amplitude problem, the Higgs boson mass is constrained to  $m_H \lesssim 1$  TeV, and if fermions acquire their masses through coupling to the Higgs boson, then  $m_H \lesssim 200$  GeV is required [3]. If the Higgs boson doesn't exist, some other form of new physics must be present at the TeV scale to prevent the  $W_L W_L$  scattering amplitude from violating the unitarity bound.

The most popular models of new physics involve without doubt supersymmetry. However, supersymmetry doesn't explain the number of fermion generations, or their mass spectrum and charges. In this talk, recent results from the Tevatron for searches for manifestations of new physics are reported, in the areas of supersymmetry, extra gauge bosons, leptoquarks, large extra dimensions, quark and lepton compositeness, the Higgs sector, and a few signature based searches. In addition, selected highlights from signature based searches at HERA are presented.

The Tevatron is a proton-antiproton collider with a collision energy of 1.96 TeV in the center of mass system. It is situated at Fermilab near Chicago. Run IIa has ended in February of 2006 with a dataset corresponding to an integrated luminosity of  $\simeq 1.3$  fb $^{-1}$  per experiment. This represents about 10 times the statistics collected in Run I. Run IIb has started in June of 2006 with the goal to reach at least 4, but possibly 8 fb $^{-1}$  by the year 2009. The two experiments DØ and CDF are by now well understood in their capabilities to detect and identify electrons, photons, muons, taus, jets of light and heavy flavours, and missing transverse energy  $\cancel{E}_T$ . The current account of delivered and recorded luminosity by DØ is shown in

Fig. 1. Only recent results based on an integrated luminosity of at least 0.3 fb $^{-1}$  are reported here. Details can be found on the corresponding experiment web sites [4].

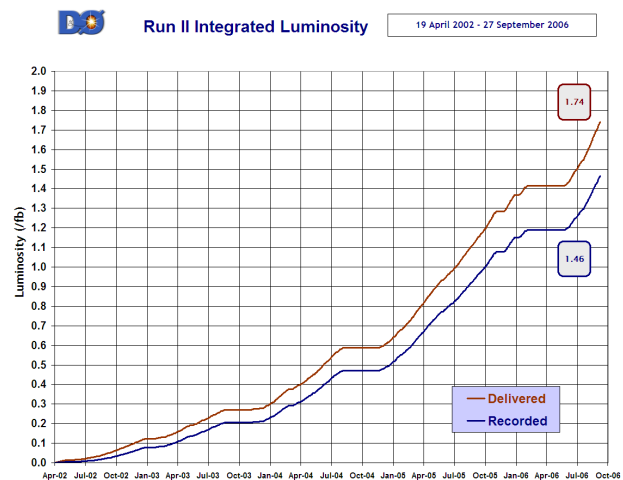


Figure 1: Integrated luminosity delivered by the Tevatron and recorded by DØ during Run II.

The HERA electron(positron)-proton collider at DESY in Hamburg has been delivering luminosity since 1992, at a center of mass energy of up to 319 GeV. HERA is currently in its “Run II” (HERA-2) as well, which started in 2002 and is expected to be completed in 2007. The total integrated luminosity accumulated by the two colliding beam experiments H1 and ZEUS for the analyses shown here is up to  $\simeq 300$  pb $^{-1}$ , with another substantial increase of the data set expected for the entire HERA data set, as can be seen for H1 in Fig. 2.

## 2. Isolated Leptons at HERA

Soon after turning on HERA, the H1 experiment reported [6] in 1994, after analyzing the first 4 pb $^{-1}$  of data, the observation of an event with an isolated muon recoiling against a hadronic system, both of high transverse momentum  $p_T$ . In addition, substantial missing transverse energy was reconstructed. The dominant SM process leading to such a final state is

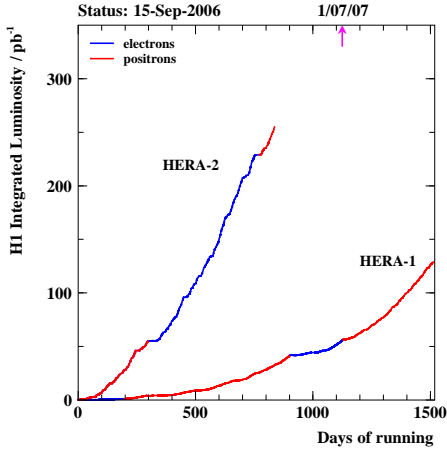


Figure 2: Integrated luminosity accumulated by the H1 detector at HERA [5].

photoproduction of  $W$  bosons with a subsequent leptonic decay of the  $W$ :  $e^+p \rightarrow e^+W^+X \rightarrow e^+\mu^+\nu X$  (Fig. 3), where the positron escapes detection and the neutrino leads to reconstructed  $\cancel{E}_T$ . However, the total cross section for this reaction is only 40 fb. In the following years, H1 has reported on the observation of more such events, in excess of the SM expectation, but not statistically significant to claim new physics.

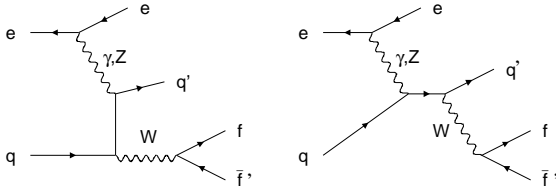


Figure 3: Main leading order Feynman diagrams for the process  $ep \rightarrow eWX$  [8].

These analyses have inspired a large number of possible interpretations in terms of physics beyond the standard model – to name a few, leptoquarks, excited fermions, supersymmetry with  $R$ -parity violation, or single top production via flavour changing neutral currents.

## 2.1. High $p_T$ Leptons and Missing $E_T$

The H1 collaboration has now updated the analysis with all data collected until the Summer of 2006, corresponding to 341  $\text{pb}^{-1}$  of data [7]. The event selection requires as before a high  $p_T$  isolated electron or muon, and substantial missing transverse momentum. The distribution of the hadronic transverse momentum  $p_T^X$ , determined from all reconstructed particles excluding identified isolated leptons, for all data com-

bined is shown in Fig. 4, with a fair agreement of data and SM expectation.

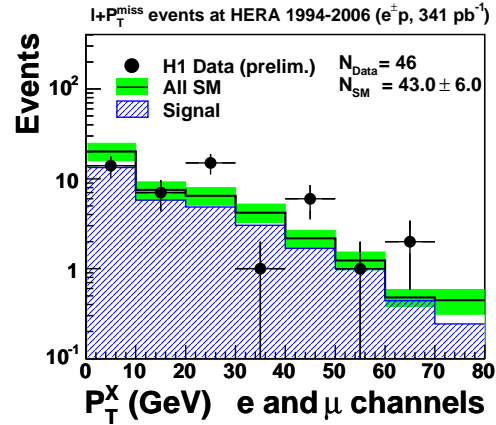


Figure 4: The hadronic transverse momentum distribution in the H1 search for isolated lepton events [7]. Electron and muon channels are combined. The SM expectation (histogram) is dominated by processes with genuine isolated leptons and missing  $E_T$  (“Signal”), which in turn is dominated by real  $W$  production.

At large hadronic transverse momentum  $P_T^X > 25$  GeV, a total of 18 events are observed compared to a SM prediction of  $11.5 \pm 1.8$ . As can be seen from Table 5, the excess is, within statistics, observed in the  $e^+p$  data only. The probability for the SM expectation to fluctuate to the observed number of events or more in the high  $P_T^X$  domain for all data is 6.7%, compared to 0.15% for the HERA I data (the majority of which is  $e^+p$  data). For the  $e^+p$  data alone, this probability is 0.03%.

H1 Preliminary		Electron obs./exp. (Signal contribution)	Muon obs./exp. (Signal contribution)	Combined obs./exp. (Signal contribution)
1994-2004 $e^+p$	Full Sample	19 / 14.6 $\pm$ 2.0 (70%)	9 / 3.9 $\pm$ 0.6 (84%)	28 / 18.5 $\pm$ 2.6 (73%)
158 $\text{pb}^{-1}$	$P_T^X > 25$ GeV	9 / 2.3 $\pm$ 0.4 (80%)	6 / 2.3 $\pm$ 0.4 (84%)	15 / 4.6 $\pm$ 0.8 (82%)
1998-2006 $e^-p$	Full Sample	16 / 19.4 $\pm$ 2.7 (65%)	2 / 5.1 $\pm$ 0.7 (78%)	18 / 24.4 $\pm$ 3.4 (68%)
184 $\text{pb}^{-1}$	$P_T^X > 25$ GeV	3 / 3.8 $\pm$ 0.6 (61%)	0 / 3.1 $\pm$ 0.5 (74%)	3 / 6.9 $\pm$ 1.0 (67%)
1994-2006 $e^\pm p$	Full Sample	35 / 34.0 $\pm$ 4.7 (68%)	11 / 9.0 $\pm$ 1.4 (80%)	46 / 43.0 $\pm$ 6.0 (70%)
341 $\text{pb}^{-1}$	$P_T^X > 25$ GeV	12 / 6.1 $\pm$ 1.1 (66%)	6 / 5.4 $\pm$ 0.9 (77%)	18 / 11.5 $\pm$ 1.8 (71%)

Figure 5: Summary [7] of the H1 results of searches for events with isolated electrons or muons and missing transverse momentum for different data sets:  $e^+p$ ,  $e^-p$ , and all data;  $e$  and  $\mu$  channel as well as combined; with and without the requirement of large hadronic transverse momentum  $p_T^X$ . The number of observed events is compared to the SM prediction. The signal component of the SM expectation, dominated by real  $W$  production, is given as a percentage in parentheses.

ZEUS has analyzed 249  $\text{pb}^{-1}$  of data taken during

the years 1998 to 2005 with a similar selection [8], and found the rate of such events at high hadronic transverse momentum to be consistent with the SM predictions (Fig. 6). The excess observed by the H1 collaboration is not confirmed. Both experiments have studied differences in the acceptances and efficiencies of the respective analyses, and reached the conclusion that the experiments have comparable sensitivity in the regions where the H1 excess is observed [7, 8].

Unfortunately, taking into account the amount of HERA data still to be analyzed in the future, it seems increasingly unlikely that the mystery of the isolated lepton events can be resolved by additional data alone.

Isolated $e$ candidates	$12 < P_T^X < 25$ GeV	$P_T^X > 25$ GeV
ZEUS (prel.) 98-99 $e^-p$ (17 pb $^{-1}$ )	1/0.23 $\pm$ 0.06 (67%)	0/0.32 $\pm$ 0.09 (65%)
ZEUS (prel.) 04-05 $e^-p$ (126 pb $^{-1}$ )	3/1.75 $\pm$ 0.36 (57%)	3/2.54 $\pm$ 0.46 (51%)
ZEUS (prel.) 99-00 $e^+p$ (66 pb $^{-1}$ )	1/1.04 $\pm$ 0.11 (57%)	1/0.92 $\pm$ 0.09 (79%)
ZEUS (prel.) 03-04 $e^+p$ (40 pb $^{-1}$ )	0/0.46 $\pm$ 0.10 (64%)	0/0.58 $^{+0.08}_{-0.06}$ (76%)
ZEUS (prel.) 98-05 $e^-p$ (143 pb $^{-1}$ )	4/1.98 $\pm$ 0.36 (58%)	3/2.86 $\pm$ 0.46 (53%)
ZEUS (prel.) 99-04 $e^+p$ (106 pb $^{-1}$ )	1/1.50 $\pm$ 0.15 (59%)	1/1.50 $^{+0.12}_{-0.13}$ (78%)
ZEUS (prel.) 98-05 $e^+p$ (249 pb $^{-1}$ )	5/3.5 $\pm$ 0.4 (58%)	4/4.4 $\pm$ 0.5 (61%)
H1 (prel.) 1994-2005 $e^\pm p$ (279 pb $^{-1}$ )	-	11/4.7 $\pm$ 0.9 (69%)

Isolated $\mu$ candidates	$12 < P_T^X < 25$ GeV	$P_T^X > 25$ GeV
ZEUS (prel.) 98-99 $e^-p$ (17 pb $^{-1}$ )	0/0.2 $\pm$ 0.02 (67%)	0/0.2 $\pm$ 0.04 (85%)
ZEUS (prel.) 04-05 $e^-p$ (126 pb $^{-1}$ )	2/1.4 $\pm$ 0.2 (68%)	2/1.4 $\pm$ 0.2 (86%)
ZEUS (prel.) 99-00 $e^+p$ (66 pb $^{-1}$ )	0/0.7 $\pm$ 0.1 (72%)	1/0.9 $\pm$ 0.2 (79%)
ZEUS (prel.) 03-04 $e^+p$ (40 pb $^{-1}$ )	1/0.5 $\pm$ 0.1 (64%)	0/0.6 $\pm$ 0.1 (82%)
ZEUS (prel.) 98-05 $e^-p$ (143 pb $^{-1}$ )	2/1.6 $\pm$ 0.2 (68%)	2/1.6 $\pm$ 0.2 (86%)
ZEUS (prel.) 99-04 $e^+p$ (106 pb $^{-1}$ )	1/1.2 $\pm$ 0.1 (69%)	1/1.5 $\pm$ 0.2 (80%)
ZEUS (prel.) 98-05 $e^+p$ (249 pb $^{-1}$ )	3/2.8 $\pm$ 0.2 (68%)	3/3.1 $\pm$ 0.3 (83%)
H1 (prel.) 1994-2006 $e^\pm p$ (341 pb $^{-1}$ )	-	6/5.4 $\pm$ 0.9 (77%)

Figure 6: Summary of the results of searches for events with isolated electrons (top) or muons (bottom) and missing transverse momentum at HERA, as shown in [8]. The number of observed events is compared to the SM prediction (observed/expected). The signal component of the SM expectation ( $W$  production) is given as a percentage in parentheses. Only the H1 results directly comparable to the ZEUS results are quoted in this Table.

## 2.2. High $p_T$ Taus and Missing $E_T$

In order to shed additional light on the question of isolated lepton production at HERA, both H1 and ZEUS have investigated the production of high  $p_T$  tau leptons. In the latest H1 analysis [9], data corresponding to an integrated luminosity of 278 pb $^{-1}$  have been used. The  $\tau$  leptons are identified by using an identification algorithm based on the search for isolated charged tracks associated to narrow hadronic jets detected in the calorimeters, a typical signature of the one-prong hadronic  $\tau$  decay. The 25 events found in the data are in good agreement with the SM expectation of  $24.2^{+4.2}_{-5.8}$  events. In the region

where the hadronic system has a transverse momentum  $P_T^X > 25$  GeV, three events are observed in the data where the SM expectation is  $0.74^{+0.19}_{-0.16}$  events. All three events have been collected in  $e^-p$  collisions, in contrast to the excess observed in the  $e$  and  $\mu$  channels. The  $p_T^X$  distribution is shown in Fig. 7.

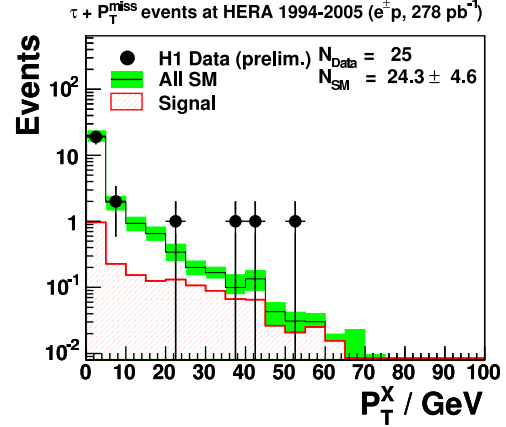


Figure 7: The hadronic transverse momentum distribution of  $\tau + \cancel{E}_T$  events in H1 data [9]. The SM expectation is shown as histogram with uncertainty band. The signal component of the SM expectation, dominated by real  $W$  production, is given by the hatched histogram.

The ZEUS collaboration has published the results of an analysis [10] of events containing isolated tau leptons and large missing transverse momentum based on 130 pb $^{-1}$  of HERA I data. For the  $\tau$  identification, six observables based on the internal jet structure were exploited to discriminate between hadronic  $\tau$  decays and quark- or gluon-induced jets. Three tau candidates were found, while  $0.40^{+0.12}_{-0.13}$  were expected from SM processes. Requiring  $P_T^X > 25$  GeV, two candidate events remain, while  $0.20 \pm 0.05$  events are expected from SM processes, about half of which is real  $W$  production. Both events occurred in  $e^+p$  collisions.

## 2.3. Events with Multiple Leptons

Both ZEUS [11] and H1 [12] have studied the production of events containing multiple high  $p_T$  isolated leptons. The dominant SM contribution to these final states is the two photon process  $\gamma\gamma \rightarrow l^+l^-$ , which can be accurately predicted. ZEUS [11] has analyzed 296 pb $^{-1}$  of data for the  $ee$  and  $eee$  final states, and compared event yields and kinematical distributions, see for example Figs. 8 and 9. Data and SM expectations are found to be in agreement. The  $\tau\tau$  final state has been analyzed in a smaller data set corresponding to 135 pb $^{-1}$ , and again no deviation from the SM prediction has been found.

The H1 collaboration has updated and extended their analysis of multi-lepton events [12], using

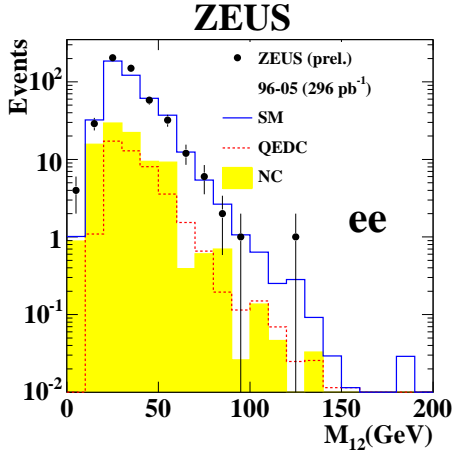


Figure 8: In the ZEUS analysis of events with two high  $p_T$  electrons [11], comparison of the observed invariant mass  $M_{12}$  of the two electrons with the SM expectation. The contributions of the QED Compton and neutral current DIS processes are also shown.

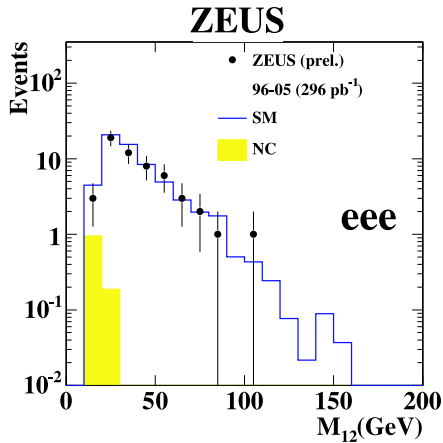


Figure 9: In the ZEUS analysis of events with three high  $p_T$  electrons [11], comparison of the observed invariant mass  $M_{12}$  of the two highest  $p_T$  electrons with the SM expectation. The contributions of the QED Compton and neutral current DIS processes are also shown.

275  $\text{pb}^{-1}$  of data. The final states  $ee$ ,  $\mu\mu$ ,  $e\mu$ ,  $eee$  and  $e\mu\mu$  have been studied for anomalies, see for example Fig. 10 for the distributions of the scalar sum  $\sum p_T$  of the lepton transverse momenta for all final states combined. For  $\sum p_T > 100$  GeV, four events are observed with a SM expectation of  $1.1 \pm 0.2$ . All four events have been collected in  $e^+p$  collisions, and three of the four events are in the  $eee$  final state and have an invariant mass of the two leading electrons of  $M_{12} > 100$  GeV. Apart from this moderate but interesting disagreement, data and SM expectation are found to be in good agreement.

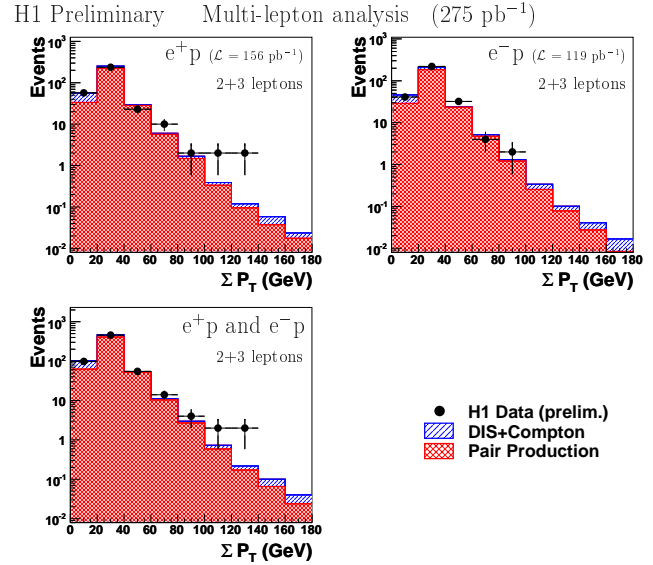


Figure 10: In the H1 analysis of events with two or three high  $p_T$  electrons or muons [12], distributions of the scalar sum of the lepton transverse momenta compared to the expectations, separately for  $e^+p$  data,  $e^-p$  data, and the entire data set.

## 2.4. Model Independent Search

The H1 collaboration has previously presented an analysis based on the HERA I data using a model independent approach to search for deviations from the standard model, reporting no significant findings. Since the HERA I data consisted mostly of  $e^+p$  data, the analysis has recently been updated with the  $e^-p$  data collected in the years 2005–2006 and corresponding to an integrated luminosity of 159  $\text{pb}^{-1}$ . Events are assigned to exclusive classes according to their final state involving isolated electrons, photons, muons, neutrinos ( $\cancel{E}_T$ ) and jets with high transverse momenta. The event yields in the different classes are shown in Fig. 11 together with the SM expectation. The  $\mu - \nu$  class has been discarded because it is dominated by poorly reconstructed muons giving rise to large  $\cancel{E}_T$ . A statistical algorithm is applied to search for deviations from the SM in the distributions of the scalar sum of transverse momenta or the invariant mass of final state particles, and to quantify their significance. No significant deviation has been found.

## 3. Supersymmetry

Supersymmetry or SUSY, a proposed invariance of nature for the interchange of fermionic and bosonic degrees of freedom, has many important features which justify an intensive research at the highest energy accelerators. It allows for the unification of the four known forces, it is the only non-trivial extension of

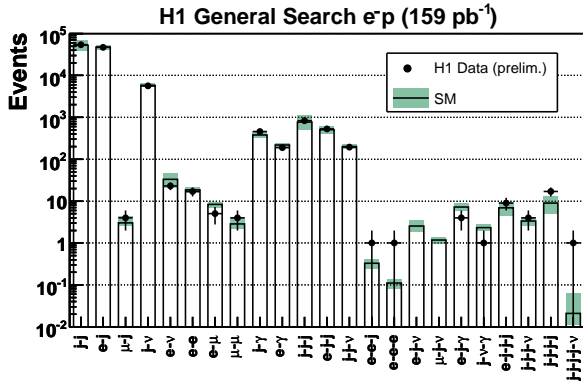


Figure 11: In the generic H1 search for deviations from the SM [13], the observed number of events in the different exclusive event classes, as well as the SM expectation with its uncertainty. Only final states with either at least one data event or a SM expectation greater than one event are shown.

the Lorentz-Poincaré group, and it provides an elegant solution to evade the fine tuning problem of the standard model. In SUSY every SM particle has a partner differing in spin  $S$  by  $1/2$ . The SUSY partners are assigned an  $R$ -parity  $R = (-1)^{3B+L+2S} = -1$ , where  $B$  is the baryon and  $L$  is the lepton number of the particle, in contrast to the SM particles of  $R = +1$ . A second Higgs doublet has to be introduced, leading to four additional Higgs particles which have  $R = +1$ . In the minimal supersymmetric extension of the SM, the MSSM, 105 additional parameters are introduced, corresponding to sparticle masses, mixing angles etc.

Since the  $R = -1$  partners have not yet been observed in nature, SUSY cannot be an exact symmetry. Various mechanisms for SUSY breaking have been proposed, each of them requiring a different set of new model parameters. Under certain assumptions the number of free parameters can be reduced to manageable numbers. In the model that is probably most studied, minimal supergravity or mSUGRA, five parameters remain: the common scalar and fermion masses at the GUT scale,  $m_0$  and  $m_{1/2}$ , the ratio of the vacuum expectation values of the two neutral Higgs fields  $\tan\beta$ , the trilinear coupling parameter  $A_0$ , and the sign of the higgsino mass parameter  $\mu$ . In the case of minimal gauge mediated SUSY breaking (mGMSB), the six parameters are  $\Lambda$ ,  $M_m$ ,  $N_5$ ,  $C_{grav}$ ,  $\tan\beta$  and the sign of  $\mu$ .

In most cases  $R$ -parity is assumed to be conserved since there are severe limits on  $B$  and  $L$  violating processes. Then, the SUSY partners are pair produced and the lightest SUSY particle (LSP) is neutral and weakly interacting, and thus escapes detection. Therefore, the basic experimental signature for  $R$ -parity conserving SUSY is missing transverse energy and multiple jets and leptons originating from the cascade decay of the heavy  $R = -1$  partners. Im-

portant SM backgrounds are  $t\bar{t}$  production and gauge boson production either in pairs or accompanied by jets. In models with  $R$ -parity conservation, the LSP, in most cases the  $\tilde{\chi}_1^0$ , is a natural dark matter candidate.

Nevertheless,  $R$ -parity violation ( $\mathcal{R}$ ) is not excluded, and remains an interesting alternative.  $\mathcal{R}$  would allow single resonant production of SUSY particles, and often even more jets or leptons in the final state from the  $B$  or  $L$  violating processes. In this case the theory contains 48 additional unknown Yukawa couplings. It is usually assumed that only one of these couplings is non-zero. At the Tevatron both  $R$ -parity conserving and  $\mathcal{R}$  processes have been studied.

### 3.1. Supersymmetry with R-Parity Conserved

The searches for SUSY under the assumption of  $R$ -parity conservation are presented as follows: searches for charginos and neutralinos, and squarks and gluinos, in mSUGRA and mSUGRA inspired scenarios, which are benchmark processes at the Tevatron. Following this, results for alternative mechanisms of SUSY breaking are discussed, including split SUSY, GMSB, and anomaly mediated SUSY breaking.

#### 3.1.1. Associated Production of Charginos and Neutralinos

The dominant production mechanisms of charginos and neutralinos at the Tevatron along with their leptonic decays are depicted in Fig. 12. The golden experimental signature searched for is three leptons, accompanied by  $\cancel{E}_T$ . For increased acceptance, the third lepton is sometimes identified as an isolated track, or not required to be found at all in the case of two leptons of same charge. The SM backgrounds ( $Z/\gamma^* + \text{jets}$ , QCD (multijets),  $WW/WZ$  and  $t\bar{t}$  production) are small and well under control already at the preselection stage, as for example seen in Fig. 13.

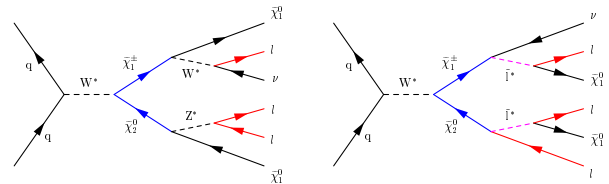


Figure 12: Dominant production of charginos and neutralinos at the Tevatron and their decays.

Because of the small leptonic branching fractions several final states need to be combined. In Table I the results in twelve different channels studied by the two collaborations are listed. Since the observed number of events is in agreement in every channel with the



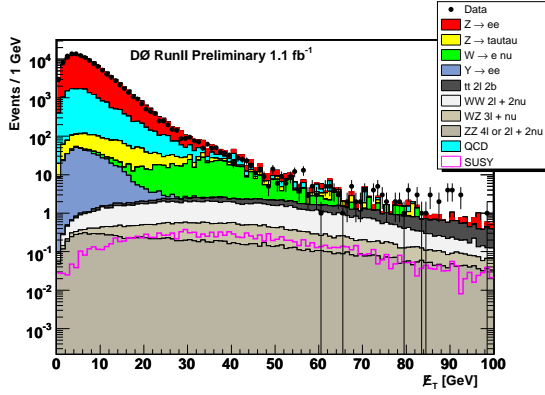


Figure 13: Distribution of  $E_T$  at the preselection stage of the “eel” chargino/neutralino search by DØ.

predicted background, upper limits on the cross section times branching fraction were derived, as shown for example in the case of DØ in Fig. 14. The theoretical predictions are for three mSUGRA inspired scenarios for mass relations as indicated in the figure. Lower limits of the chargino mass have been derived for two scenarios with large leptonic branching fractions:  $m(\tilde{\chi}_1^\pm) < 140$  GeV is excluded when the slepton mass is slightly above the mass of the second neutralino, thus allowing only 3-body decays (denoted “3l-max”), and  $m(\tilde{\chi}_1^\pm) < 154$  GeV is excluded for the case when squarks are heavy and therefore the destructive  $t$ -channel contribution is minimal. The CDF analyses have comparable sensitivity. The slight excess in the CDF same sign dilepton channel is worth noting, because it turns out that four of the nine events have a leading lepton with high transverse momentum in excess of 60 GeV, where neither SM background nor the SUSY signal are expected (Fig. 15).

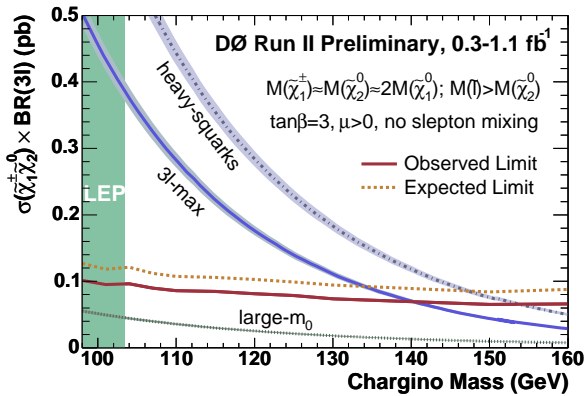


Figure 14: Cross section upper limits times branching fraction of chargino and neutralino production measured by DØ along with theoretical predictions.

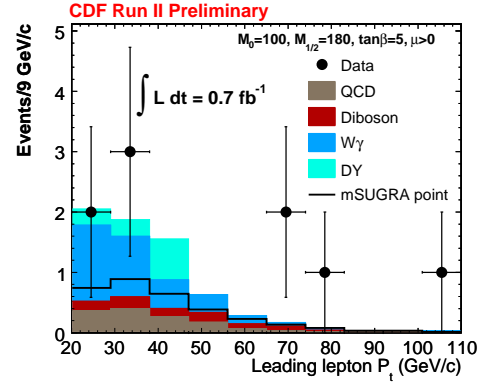


Figure 15: Transverse momentum of the leading lepton in the CDF search for charginos and neutralinos in like sign dileptons.

DØ channels	$\mathcal{L}_{\text{int}}$ [ $\text{fb}^{-1}$ ]	Background	Data
$ee + \text{track}$	1.1	$0.76 \pm 0.67$	0
$\mu\mu + \text{track}$	0.32	$1.75 \pm 0.57$	2
$e\mu + \text{track}$	0.32	$0.31 \pm 0.13$	0
$\mu^+\mu^+ / \mu^-\mu^-$	0.9	$1.1 \pm 0.4$	1
$e\tau + \text{track}$	0.33	$0.58 \pm 0.14$	0
$\mu\tau + \text{track}$	0.33	$0.36 \pm 0.13$	1
CDF channels	$\mathcal{L}_{\text{int}}$ [ $\text{fb}^{-1}$ ]	Background	Data
$ee + e/\mu$	0.35	$0.17 \pm 0.05$	0
$ee + \text{track}$	0.61	$0.49 \pm 0.10$	1
$\mu\mu + e/\mu$ (low $p_T$ )	0.31	$0.13 \pm 0.03$	0
$\mu\mu + e/\mu$ (high $p_T$ )	0.75	$0.64 \pm 0.18$	1
$e\mu + e/\mu$	0.75	$0.78 \pm 0.11$	0
$e^\pm e^\pm, e^\pm \mu^\pm, \mu^\pm \mu^\pm$	0.70	$6.8 \pm 1.0$	9

Table I Three and two lepton final states studied by the DØ and CDF collaborations in the search for charginos and neutralinos.

### 3.1.2. Squarks and Gluinos

DØ has carried out a generic search [14] for gluinos and squarks requiring a minimum number of jets,  $N_j$ , accompanied by substantial  $\cancel{E}_T$  and  $H_T$ , the scalar sum of the jet transverse energies, for the following three topologies: (i)  $N_j = 2$  for  $M_{\tilde{q}} < M_{\tilde{g}}$ , (ii)  $N_j = 3$  for  $M_{\tilde{q}} \simeq M_{\tilde{g}}$ , and (iii)  $N_j = 4$  for  $M_{\tilde{q}} > M_{\tilde{g}}$ , where  $M_{\tilde{q}}$  and  $M_{\tilde{g}}$  are the mass of the squark and the mass of the gluino, respectively, and the jet multiplicities are chosen corresponding to the decay modes  $\tilde{q} \rightarrow q\tilde{\chi}_1^0$  and  $\tilde{g} \rightarrow q\tilde{q}\tilde{\chi}_1^0$ . A general agreement between the data corresponding to an integrated luminosity of  $310 \text{ pb}^{-1}$  and the expected background at all stages of the selection is observed, for the DØ analyses as well as for the CDF analysis in the 3-jet final state, as can be seen for example in Fig. 16, where the CDF  $H_T$  distribution optimized to search for relatively small gluino masses is displayed. The three DØ analyses

optimized for the three different mass hierarchies are combined, and the exclusion region in the  $(M_{\tilde{q}}, M_{\tilde{g}})$  plane as shown in Fig. 17 is obtained. Also shown is the excluded region obtained by CDF using the 3-jet event topology and 371 pb<sup>-1</sup> of data. The absolute lower mass limits at 95% C.L. are  $M_{\tilde{q}} > 325$  GeV and  $M_{\tilde{g}} > 241$  GeV, while for  $M_{\tilde{q}} \simeq M_{\tilde{g}}, M_{\tilde{q},\tilde{g}} < 387$  GeV can be excluded.

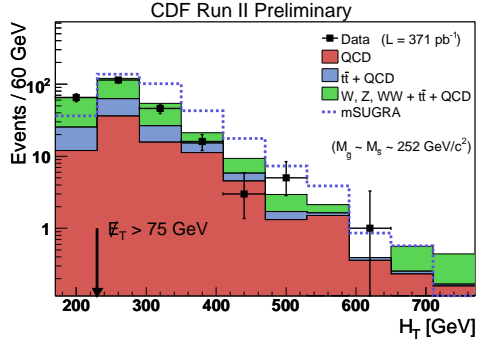


Figure 16: Distribution of  $H_T$  obtained by CDF for the 3-jet event topology and a light gluino, compared with the SM background and the expected SUSY signal.

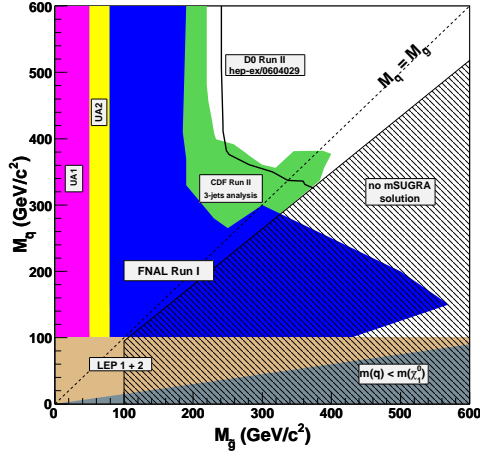


Figure 17: Excluded regions in the  $(M_{\tilde{q}}, M_{\tilde{g}})$  plane obtained by CDF and DØ. It should be noted that DØ has used conservatively a theoretical cross section reduced by its uncertainty when calculating limits.

Third generation squarks may be light due to the large mixing between the scalar partners of the left and right handed quarks. They may be accessible at the Tevatron and are therefore subject of dedicated analyses by the two collaborations.

Both DØ [15] ( $\mathcal{L}_{\text{int}} = 310$  pb<sup>-1</sup>) and CDF (295 pb<sup>-1</sup>) have searched for direct pair production of the lightest sbottom quark  $\tilde{b}_1$ , assuming that it decays with a branching fraction of 100% into a  $b$  quark and the lightest neutralino. The experimental signa-

ture is two acoplanar  $b$  jets and  $\cancel{E}_T$ . In both analyses at least one of the jets was required to be identified as a  $b$  jet using lifetime information. The selection value of the  $\cancel{E}_T$  and that of the  $E_T$  of the jets were optimized according to the mass value of the sbottom to be detected. The data did not show any significant excess over the expected SM background as can be seen for example in Fig. 18, where the  $\cancel{E}_T$  distribution obtained by CDF is shown. The excluded mass values of the sbottom and the neutralino are shown in Fig. 19, substantially improving on previous limits.

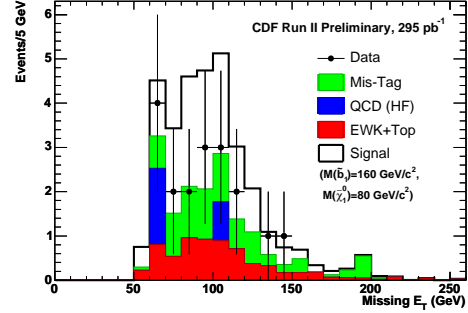


Figure 18: Distribution of  $\cancel{E}_T$  in events with at least one  $b$ -tagged jet observed by CDF in the search for sbottom pair production with  $\tilde{b} \rightarrow b\tilde{\chi}_1^0$ , together with the SM background and the expected signal.

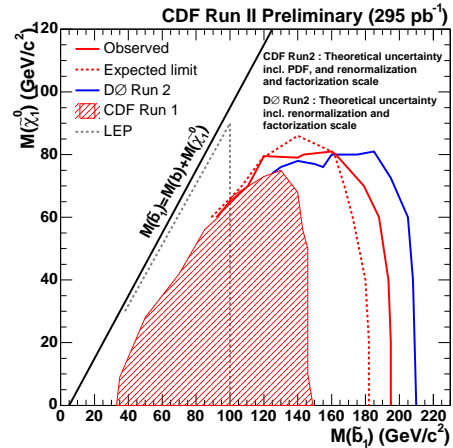


Figure 19: Mass values of the sbottom and neutralino excluded by the DØ and CDF analyses of sbottom pair production followed by the decay  $\tilde{b} \rightarrow b\tilde{\chi}_1^0$ .

If the mass  $M_{\tilde{t}_1}$  of the lightest stop quark  $\tilde{t}_1$  satisfies the relation  $M_c + M_{\tilde{\chi}_1^0} < M_{\tilde{t}_1} < M_b + M_W + M_{\tilde{\chi}_1^0}$ , where  $M_c$ ,  $M_b$ ,  $M_{\tilde{\chi}_1^0}$  and  $M_W$  are the masses of the  $c$  quark, the  $b$  quark, the lightest neutralino and the  $W$  boson, respectively, its dominant decay mode is  $\tilde{t}_1 \rightarrow c\tilde{\chi}_1^0$ , and a similar search strategy can be applied as for the sbottom analysis outlined above, ex-

cept that jets should satisfy a  $c$ -tag instead of a  $b$ -tag criterion. Again, data observed by  $D\bar{O}$  and by CDF are in agreement with the SM expectation (see for example Fig. 20), and exclusion limits can be set in the mass plane of the lightest stop and the neutralino, extending the previously excluded regions of  $M_{\tilde{t}_1}$  and  $M_{\tilde{\chi}_1^0}$ , as shown in Fig. 21.

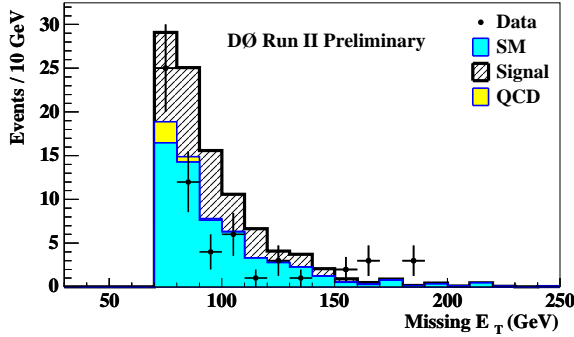


Figure 20: Final  $E_T$  distribution in events with at least one  $c$ -tagged jet observed by  $D\bar{O}$  in the search for stop pair production with  $\tilde{t} \rightarrow c\tilde{\chi}_1^0$ , together with the SM background and the expected signal for  $M_{\tilde{t}_1} = 130$  GeV and  $M_{\tilde{\chi}_1^0} = 50$  GeV.

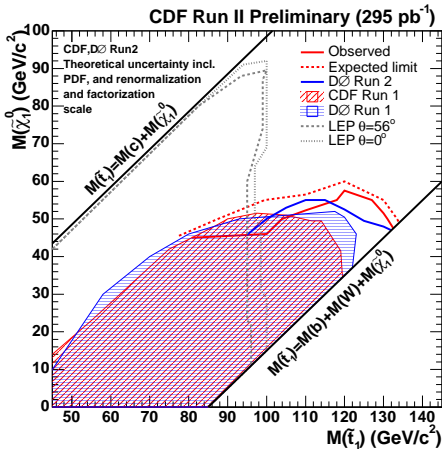


Figure 21: Mass values of the lightest stop and neutralino excluded by the  $D\bar{O}$  and CDF analyses of stop pair production followed by the decay  $\tilde{t} \rightarrow c\tilde{\chi}_1^0$ .

$D\bar{O}$  has also searched for pair production of  $\tilde{t}_1$  quarks assuming that they decay into a  $b$  quark, a lepton and a sneutrino via a virtual chargino, which may be favorable due to the relatively weak constraint on the sneutrino mass from LEP,  $M_{\tilde{\nu}} > 43.7$  GeV. The final state is two isolated leptons with opposite charge, two  $b$  jets, and  $E_T$ . For the two leptons, the combinations  $\mu\mu$  and  $e\mu$  have been analyzed. While in the  $\mu\mu$  analysis a  $b$  jet is required to be identified, the  $e\mu$  analysis has smaller backgrounds and requires

a certain number of non-isolated tracks instead of an explicit jet reconstruction, thus increasing the sensitivity. In neither channel a significant signal for the presence of the  $\tilde{t}_1$  quark has been observed. Therefore, the two analyses have been combined to exclude masses of the  $\tilde{t}_1$  quark and the sneutrino. The mass region excluded by earlier experiments has been significantly extended, as can be seen in Fig. 22.

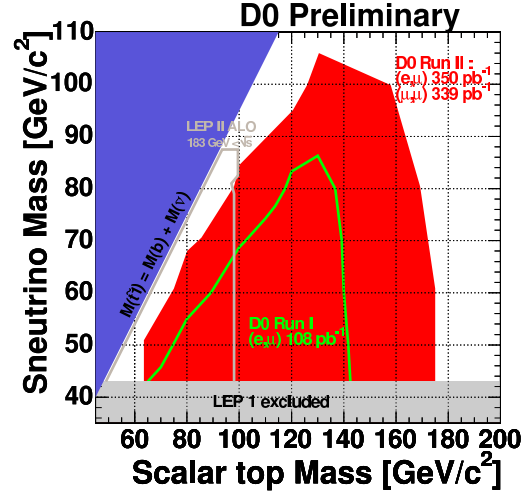


Figure 22: Excluded regions of the stop and sneutrino masses obtained by  $D\bar{O}$  assuming the decay  $\tilde{t}_1 \rightarrow b + l + \tilde{\nu}$  ( $l = e, \mu$ ).

### 3.1.3. Split SUSY

Split SUSY is a relatively new variant of supersymmetry in which the supersymmetric scalars are heavy (possibly GUT scale) compared to the (SUSY) fermions [16]. It avoids much of the fine tuning required to remain consistent with observations while still preserving the favored consequences: a dark-matter candidate is still present in the theory to explain the observed cold dark matter density in the universe, and coupling unification at the GUT scale still occurs. Due to the high masses of the scalars, the gluinos decays are suppressed. The gluinos have time to hadronize into “R-hadrons”, colorless bound states of a gluino and other quarks or gluons. At the Tevatron, R-hadrons could be pair produced copiously through strong interactions. About half of the R-hadrons are expected to be charged, and some charged R-hadrons can become “stopped gluinos” by losing all of their momentum through ionization and coming to rest in the calorimeters. Their decays may happen after several bunch crossings.

$D\bar{O}$  has searched for stopped gluinos in the  $\tilde{g} \rightarrow g\tilde{\chi}_1^0$  decay channel by looking for randomly oriented jets in bunch crossings without an inelastic  $p\bar{p}$  collision. The background consists mainly of cosmic and beam



halo muon induced jets where the muon escapes reconstruction. It has been estimated using the data. The energy distribution of the observed jets is shown in Fig. 23, along with that of the estimated background. As can be seen the data do not show any excess above the expected background. The derived cross section upper limits are shown in Fig. 24 as a function of the gluino mass for different mass values of the  $\tilde{\chi}_1^0$ . The theoretical cross section is also shown, from which gluino masses below  $\simeq 300$  GeV can be excluded if the mass of the  $\tilde{\chi}_1^0$  is less than 90 GeV. It is worth noting that the signature of a long-lived gluino could occur in many models of beyond the standard model physics.

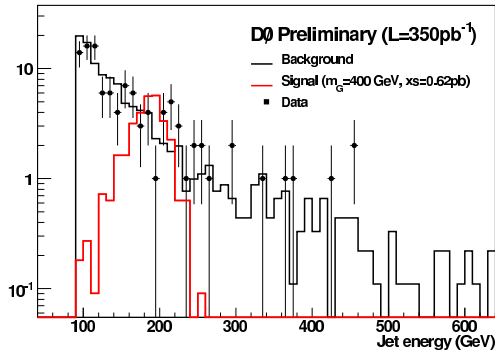


Figure 23: In the  $D\emptyset$  search for stopped gluinos, energy distribution of the selected jets (dots with error bars), of the background (black histogram) – dominated by cosmic muon events –, and of a gluino of mass 400 GeV decaying into a gluon and a neutralino of 90 GeV mass.

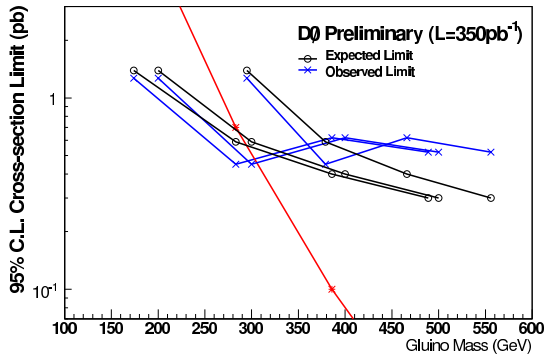


Figure 24: Expected and observed cross section upper limits from  $D\emptyset$  for stopped gluinos as a function of the gluino mass for neutralino masses of 50 GeV, 90 GeV and 200 GeV. Also shown is the theoretical cross section (red star).

### 3.1.4. Gauge Mediated SUSY Breaking

In the mGMSB scenario, the gravitino is the LSP with a mass less than  $\sim 1$  keV, and the next-to-lightest SUSY particle (NLSP) may be the lightest neutralino, which decays to a gravitino and a photon. The lifetime of the NLSP is a priori unknown and depends on the  $C_{grav}$  parameter of the model.  $D\emptyset$  and CDF have searched for two highly energetic prompt photons accompanied by large  $\cancel{E}_T$ , caused by the undetected gravitino. As can be seen in Fig. 25, the observed  $\cancel{E}_T$  distribution is compatible with the SM background. With recent data corresponding to  $760 \text{ pb}^{-1}$ ,  $D\emptyset$  has improved the previous limits obtained from combined measurements of CDF and  $D\emptyset$ , see Fig. 26. For the  $\Lambda$  parameter, determining the effective scale of SUSY breaking,  $\Lambda < 88.5$  TeV is excluded at 95% C.L. This corresponds to a  $\tilde{\chi}_1^0$  mass of  $> 120$  GeV and a  $\tilde{\chi}_1^\pm$  mass of  $> 220$  GeV.

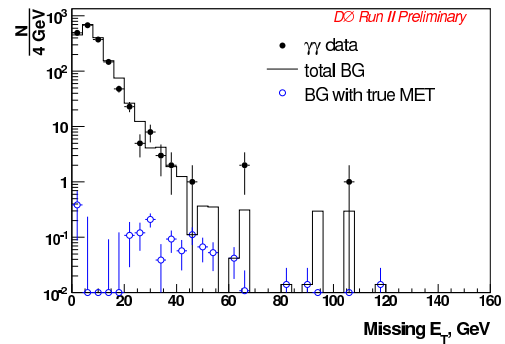


Figure 25: In events with two photons,  $\cancel{E}_T$  distribution of recent  $D\emptyset$  data (full circles), of the background (histogram), and the fraction of the latter with true  $\cancel{E}_T$  (open circles).

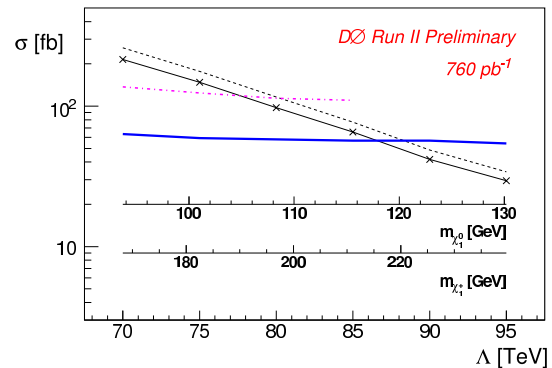


Figure 26: Cross section upper limits (solid blue line) in the  $D\emptyset$  GMSB analysis with two photons and  $\cancel{E}_T$ . The theoretical LO (NLO) cross section for the GMSB process (solid (dashed) black lines) corresponds to the SUSY Snowmass slope 8, with a messenger mass  $M_m = 2\Lambda$ , the number of messengers  $N_5 = 1$ ,  $\tan \beta = 15$ , and  $\mu > 0$ .

CDF searched for signs of GMSB assuming long lifetime for the NLSP, i.e. the neutralino, by looking for “late” photons in the calorimeter, using  $570 \text{ pb}^{-1}$  of data. Fig. 27 shows that the arrival time distribution of photons accompanied by  $\cancel{E}_T$  doesn’t show a significant excess at positive times where the GMSB signal is expected. Ten events are observed with  $7.6 \pm 1.9$  background events expected. This allows to exclude a region in the plane of the neutralino lifetime versus the neutralino mass, as shown in Fig. 28.

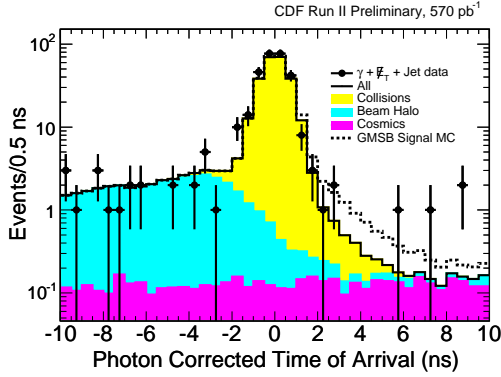


Figure 27: Photon arrival time distribution in the CDF electromagnetic calorimeter. The expected GMSB signal is for a neutralino mass of 93.6 GeV with a lifetime of 10 ns.

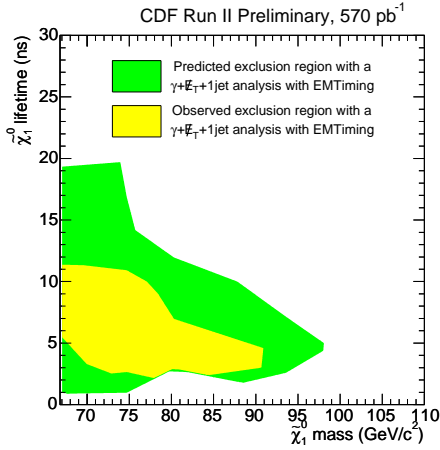


Figure 28: Excluded mass and lifetime values of the lightest neutralino (NLSP) in the CDF GMSB analysis with late photons.

### 3.1.5. Anomaly Mediated SUSY Breaking

Many SUSY scenarios contain charged massive long-lived particles expected to traverse the entire detector, for example staus or charginos with long lifetime. DØ has studied chargino pair production assuming anomaly mediated supersymmetry breaking. In this case the mass difference of the lightest

chargino and neutralino is expected to be small, less than  $\simeq 150 \text{ MeV}$ . Therefore charginos can have a long lifetime, and leave a muon-like signature in the detector. However, due to their mass they move slowly, and the speed significance, defined as  $s = (1-v)/\sigma_v$ , where  $v$  is the speed of the chargino in units of the speed of light as measured in the muon system and  $\sigma_v$  is its uncertainty, is shifted towards positive values depending on the mass, as indicated in Fig. 29 for heavy staus. In the DØ analysis of  $390 \text{ pb}^{-1}$  of data, two muons with  $s > 0$  were required, and a final optimized cut was placed in the plane of the dimuon invariant mass and  $s$ . The observed number of events is compatible with the expected background, estimated from muon pairs from the  $Z \rightarrow \mu^+\mu^-$  decay. An upper limit of the production cross section was derived (Fig. 30) which, by confronting it with the theoretical cross section, excludes wino-like charginos with a mass of less than 174 GeV.

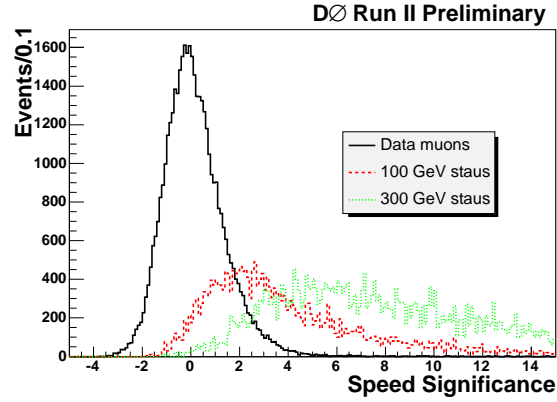


Figure 29: Speed significance distributions of muons and of long-lived staus for two different masses. The distributions are expected to be similar for charginos of the same mass.

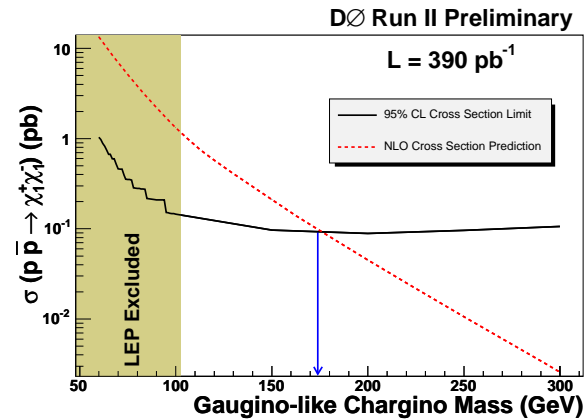


Figure 30: Cross section upper limit obtained by DØ and theoretical cross section for a gaugino-like chargino as a function of its mass.

### 3.2. R-Parity Violation

While in many analyses  $R$ -parity is assumed to be conserved, which leaves the lightest supersymmetric particle (LSP) stable, SUSY does not require  $R$ -parity conservation. If  $\mathcal{R}$  is allowed, the following trilinear and bilinear terms appear in the superpotential [17]:

$$W_{\mathcal{R}} = +\frac{1}{2}\lambda_{ijk}L_iL_j\bar{E}_k + \lambda'_{ijk}L_iQ_j\bar{D}_k \\ +\frac{1}{2}\lambda''_{ijk}\bar{U}_i\bar{D}_j\bar{D}_k + \mu_iL_iH_u$$

where  $L$  and  $Q$  are the lepton and quark SU(2) doublet superfields,  $\bar{E}$ ,  $\bar{U}$ ,  $\bar{D}$  denote the singlet fields, and  $i, j, k$  refer to the fermion families. The first two terms imply lepton number violation, while the third term leads to baryon number violation. The coupling strengths are given by the Yukawa coupling constants  $\lambda$ ,  $\lambda'$  and  $\lambda''$ . The last term,  $\mu_iL_iH_u$ , mixes the lepton and the Higgs superfields. The  $\lambda$  and  $\lambda'$  couplings give rise to final states with multiple leptons, which provide excellent signatures at the Tevatron. Stringent limits exist on the size of many  $\mathcal{R}$  couplings [18, 19], in particular for the case of more than one non-zero coupling.

#### 3.2.1. Gaugino Production in Multi Lepton Final States

The charginos and neutralinos are produced in pairs or associated and with  $R$ -parity conserved. The produced sparticles (cascade) decay to the lightest neutralino  $\tilde{\chi}_1^0$ . Under the assumption of a single non-zero  $LL\bar{E}$  coupling, the neutralino decays into two charged leptons and one neutrino by violating  $R$ -parity (Fig. 31). The final state therefore contains at least four charged leptons and two neutrinos which lead to missing transverse energy in the detector.

Both DØ and CDF have searched for this signature, assuming a sufficiently large  $LL\bar{E}$  coupling leading to a prompt decay of the lightest neutralino, i.e. the corresponding  $LL\bar{E}$ -coupling ( $\lambda_{121}$ ,  $\lambda_{122}$ , or  $\lambda_{133}$ ) has to be larger than  $\gtrsim 0.01$ . In the DØ analysis [20], based on  $360 \text{ pb}^{-1}$  of data, for best acceptance only three

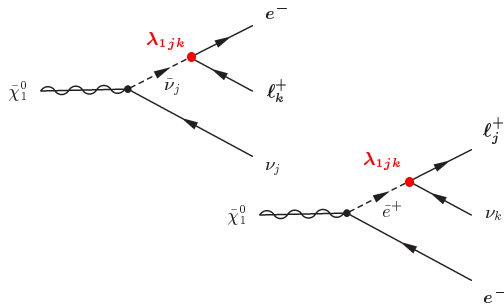


Figure 31: Two examples of  $\mathcal{R}$ -decays of the lightest neutralino via the  $LL\bar{E}$  couplings  $\lambda_{1jk}$ . In each decay, two charged leptons and one neutrino are produced.

charged leptons are required to be identified. Three different analyses  $eel$ ,  $\mu\mu l$  and  $ee\tau$  with  $l = e, \mu$  are performed depending on the flavors of the leptons in the final state. All three analyses are optimized separately using SM and signal Monte Carlo simulations. After all cuts, no events remain in the data, while  $0.9 \pm 0.4$ ,  $0.4 \pm 0.1$ , and  $1.3 \pm 1.8$  events are expected from SM processes in the  $eel$ ,  $\mu\mu l$ , and  $ee\tau$  analysis, respectively. The dominant SM backgrounds are due to  $Z/\gamma^* \rightarrow l^+l^-$  and diboson production.

Since no evidence for  $\mathcal{R}$ -SUSY is observed, the analyses are combined and upper limits on the chargino and neutralino pair production cross section are set. Lower bounds on the masses of the lightest neutralino and the lightest chargino are derived in mSUGRA and in an MSSM scenario with heavy sfermions, but assuming no GUT relation between  $M_1$  and  $M_2$ . The limits as shown in Figs. 32 and 33 are the most restrictive to date. CDF has shown preliminary results with comparable sensitivity.

#### 3.2.2. Long-Lived Neutral Particles in Dimuon Final States

In this DØ analysis [21], a small  $LL\bar{E}$  coupling  $\lambda_{122}$  is assumed, leading to a long neutralino  $\tilde{\chi}_1^0$  lifetime and consequently to a displaced dimuon vertex. The final state is of particular interest due to an anomaly reported by the NuTeV collaboration; in 2000, NuTeV reported [22] on a search for heavy neutral leptons decaying to  $\mu\mu\nu$ , amongst other final states. In the dimuon channel, they observed three events while only 0.07 events were expected. Because of the asymmetry in the muon momenta, and the absence of a signal in other channels, NuTeV argued that the signal was unlikely to be due to neutral heavy leptons.

To shed light on the origin of these events, DØ has searched for pairs of oppositely charged isolated muons originating from a common vertex located be-

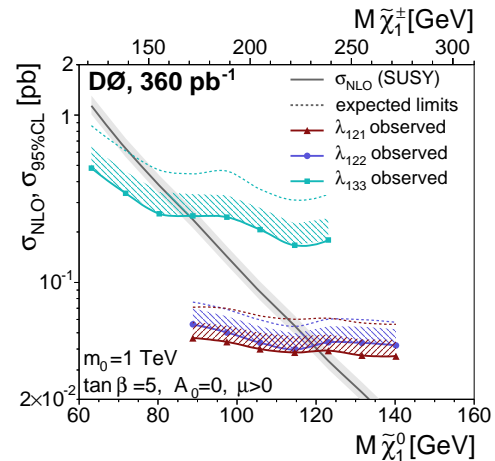


Figure 32: Cross section limits from DØ for three different  $LL\bar{E}$  couplings compared to the mSUGRA cross section prediction.

tween 5 and 20 cm radially displaced from the beamline. In this region, a good calibration using  $K_S$  mesons is possible. No events have been found in  $380 \text{ pb}^{-1}$  of data, with an estimated background of  $0.8 \pm 1.6$  events. The result is interpreted as cross section upper limit on the production times branching fraction of a neutral long-lived particle decaying into  $\mu^+\mu^- + X$  as a function of its lifetime, as shown in Fig. 34. To compare with the NuTeV result, the momentum of the hypothetical new particles in the neutrino beam was converted to the Tevatron center of mass frame. While the result is somewhat dependent on the assumptions made regarding the decay of the long-lived particle, this result excludes an interpretation of the NuTeV excess of dimuon events in a large class of models.

### 3.2.3. Resonant Second Generation Slepton Production

The  $LQ\bar{D}$  coupling offers the opportunity to produce sleptons in  $p\bar{p}$  collisions as resonances. For a non-zero coupling  $\lambda'_{211}$  this is either a smuon or a muon sneutrino. The slepton cascade decays into the lightest neutralino  $\tilde{\chi}_1^0$  and associated leptons. The neutralino decays via the same  $R$ -parity violating coupling  $\lambda'_{211}$  into a 2<sup>nd</sup> generation lepton and two jets. The cross section is proportional to  $(\lambda'_{211})^2$ , so that limits on this coupling can be derived.

DØ has recently published [23] the results of a search for resonant second generation slepton production. The three channels (i)  $\tilde{\mu} \rightarrow \tilde{\chi}_1^0 \mu$ , (ii)  $\tilde{\mu} \rightarrow \tilde{\chi}_{2,3,4}^0 \mu$ , and (iii)  $\tilde{\nu}_\mu \rightarrow \tilde{\chi}_{1,2}^\pm \mu$  resulting in dimuon and multijet final states are analyzed separately. For the further discrimination of the signal and the SM background, the analysis makes use of the possibility to reconstruct the neutralino and the slepton masses: using the leading muon and the two leading jets one

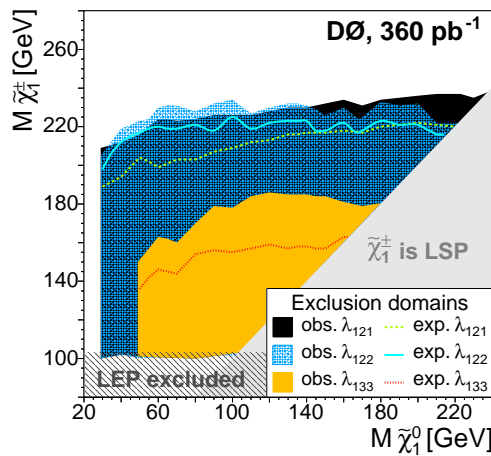


Figure 33: Exclusion contours for the three  $L\bar{L}\bar{E}$  couplings  $\lambda_{121}$ ,  $\lambda_{122}$ ,  $\lambda_{133}$  in the  $m(\tilde{\chi}_1^0)$ - $m(\tilde{\chi}_1^\pm)$  plane for an MSSM scenario without mass unification of  $M_1$  and  $M_2$ .

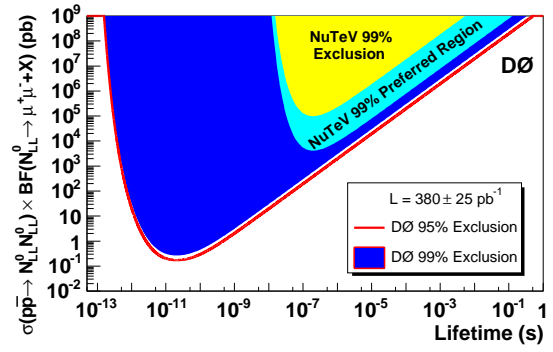


Figure 34: Cross section upper limits times branching fraction for neutral long-lived particles decaying to muon pairs as a function of their lifetime.

would be able to reconstruct the lightest neutralino, and a peak in the invariant mass of the two muons and all jets would indicate the presence of the slepton. The selection criteria are optimized depending on the slepton and neutralino mass, and for all 117 mass combinations being probed, the data corresponding to  $380 \text{ pb}^{-1}$  show no excess with respect to the SM expectation.

In the absence of an excess in the data, cross section limits on resonant slepton production were set. The results are interpreted within the mSUGRA framework with  $\tan \beta = 5$ ,  $\mu < 0$  and  $A_0 = 0$ , and an exclusion contour as a function of  $\lambda'_{211}$  is derived after combination of all three channels, as shown in Fig. 35. Lower limits for the slepton mass of 210, 340 and 363 GeV are obtained for  $\lambda'_{211}$  values of 0.04, 0.06 and 0.10, respectively, a significant improvement compared to previous results.

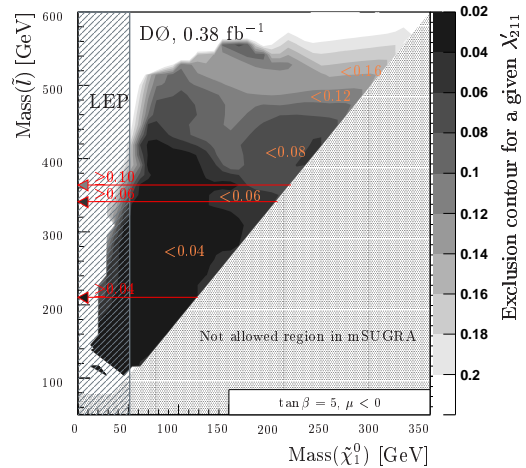


Figure 35: Cross section upper limits for the slepton mass versus the neutralino mass obtained in the DØ search for  $\tilde{R}$  SUSY with a non-zero  $\lambda'_{211}$  coupling.

### 3.2.4. Resonant Sneutrino Production

Here, a  $\tilde{\nu}_\tau$  is produced with a  $\lambda'_{311}$  Yukawa coupling which subsequently decays to an oppositely charged electron-muon pair via a non-zero  $\lambda_{132}$  coupling (Fig. 36). If such a process existed, a peak in the electron-muon invariant mass would be seen. CDF searched for such electron-muon pairs in  $344 \text{ pb}^{-1}$  of data, but has seen no indication for an enhancement in their mass distribution (Fig. 37). Therefore exclusion limits as a function of the  $\tilde{\nu}_\tau$  mass and the two Yukawa couplings are derived as shown for example in Fig. 38.

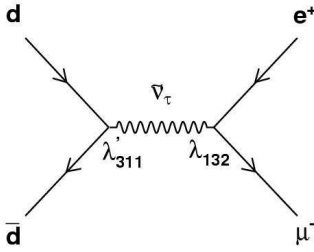


Figure 36: Production and decay of a tau sneutrino  $\tilde{\nu}_\tau$  involving two different  $R$  couplings.

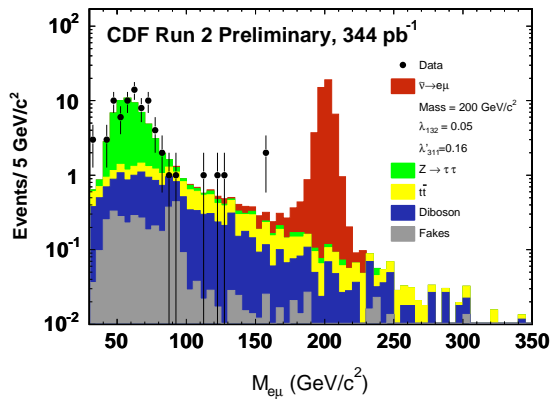


Figure 37: Invariant mass distribution of the electron-muon pairs in the CDF search for resonant tau sneutrino production.

### 3.2.5. Stop Pair Production

CDF has searched for pair production of stop quarks where both of them decay promptly into a  $b$  quark and a  $\tau$  via the  $R$ -parity violating non-zero  $\lambda'_{333}$  coupling, and one of the taus decays leptonically, the other one into hadrons. In  $322 \text{ pb}^{-1}$  of data, two events have been found with an isolated electron (or muon), a hadronic tau decay and two additional jets, whereas  $2.26^{+0.46}_{-0.22}$  SM background events are expected. The derived upper limit of cross section times

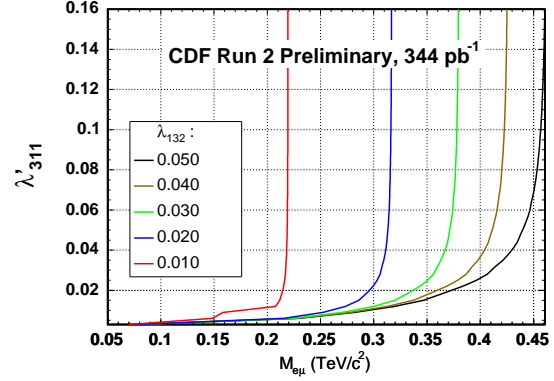


Figure 38: Excluded regions in the plane  $\lambda'_{311}$  versus the mass of the  $\tilde{\nu}_\tau$ , obtained by CDF.

branching fraction as a function of the stop mass, together with the theoretical expectation, is displayed in Fig. 39. A lower limit of 155 GeV for the stop mass has been obtained, assuming 100% branching fraction for the decay  $\tilde{t}_1 \rightarrow b + \tau$ .

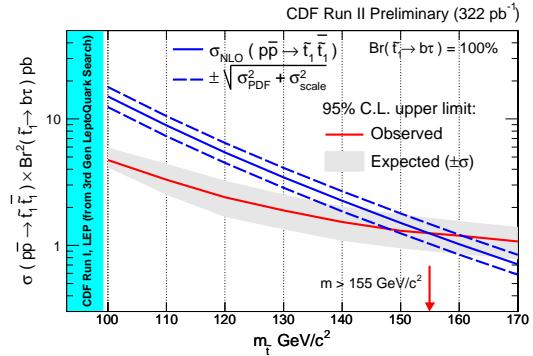


Figure 39: Upper limits of cross section times branching fraction as a function of the stop mass obtained by CDF assuming the decay  $\tilde{t}_1 \rightarrow b + \tau$ . Also shown is the theoretical expectation.

## 3.3. Search for MSSM Higgs

In models of electroweak symmetry breaking with two Higgs doublets, such as the MSSM, there are five physical Higgs bosons: two neutral  $CP$ -even scalars,  $h$  and  $H$ , a neutral  $CP$ -odd state,  $A$ , and two charged states,  $H^\pm$ . Neutral Higgs bosons are generically denoted as  $\phi$ . At tree level, the Higgs sector of the MSSM is fully specified by two parameters, generally chosen to be  $M_A$ , the mass of the  $CP$ -odd Higgs boson, and  $\tan \beta$ . At large  $\tan \beta$ , the coupling of the neutral Higgs bosons to down-type quarks and charged leptons is strongly enhanced, leading to sizeable cross sections. In this region, the  $A$  boson is nearly degener-



ate in mass with the  $h$  or the  $H$  boson. The dominant decay modes are  $\phi \rightarrow b\bar{b}$  ( $\simeq 90\%$ ) and  $\phi \rightarrow \tau^+\tau^-$  ( $\simeq 8\%$ ), and the most promising search channels are considered to be either in association with  $b$  quarks,  $\phi b(\bar{b}) \rightarrow b\bar{b}b(\bar{b})$ , or  $\phi \rightarrow \tau^+\tau^-$ .

CDF has published results of a search for neutral supersymmetric Higgs bosons in the decay to  $\tau^+\tau^-$  [24], based on  $310 \text{ pb}^{-1}$  of data, and  $D\mathcal{O}$  published [25] results both in the  $\tau^+\tau^-$  channel as well as for the decay into  $b\bar{b}$  in association with  $b$  quarks, leading to final states with three or four  $b$  jets, using integrated luminosities of  $325 \text{ pb}^{-1}$  and  $260 \text{ pb}^{-1}$ , respectively. In the  $\tau^+\tau^-$  channel, both experiments require one of the taus to decay leptonically, and the other one hadronically; in addition,  $D\mathcal{O}$  uses the  $e\mu$  channel. The main discriminating variable in the search is the visible mass  $M_{vis}$ , calculated from the partially reconstructed tau decays. The dominant background is from  $Z/\gamma^* \rightarrow \tau^+\tau^-$  decays.

Searching for a MSSM Higgs in the decay into  $b\bar{b}$  in association with  $b$  quarks, the signal would show up in the dijet invariant mass distribution of the two leading jets. To suppress the dominant multijet background,  $D\mathcal{O}$  requires at least three jets with  $b$  quarks identified by a secondary vertex algorithm.

In neither of the analyses a significant excess has been found, and exclusion limits are derived in the  $(M_A, \tan\beta)$  plane. All results are summarized for one of the benchmark scenarios [26], the “no-mixing” scenario, in Fig. 40. With increasing amounts of data, these analyses impose more and more stringent constraints on the MSSM Higgs sector.

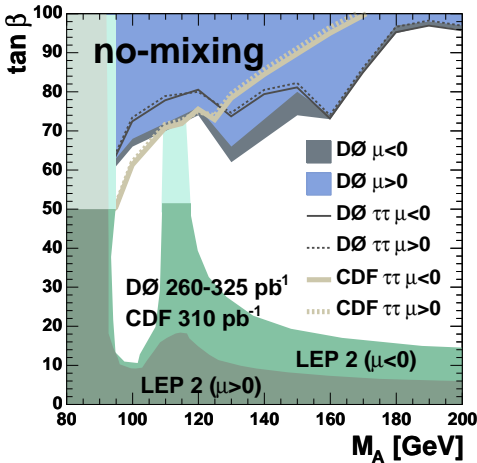


Figure 40: Excluded region in the  $(M_A, \tan\beta)$  plane for the “no-mixing” scenario [26] for  $\mu = -0.2 \text{ TeV}$  and  $\mu = +0.2 \text{ TeV}$ . The regions labeled “ $D\mathcal{O} \mu < 0$ ” and “ $D\mathcal{O} \mu > 0$ ” refer to the combination of the  $D\mathcal{O} \tau^+\tau^-$  and multijet analyses.

## 4. New Gauge Bosons

A possible way of resolving the inherent problems of the standard model is by extending the gauge sector of the theory. New heavy gauge bosons are predicted in many extensions of the standard model. For example, in little Higgs models, the quadratically divergent radiative corrections to the Higgs mass are canceled individually, leading to the appearance of partners of the  $W$  and  $Z$  bosons at the TeV scale. In grand unified theories heavy partners of the electroweak bosons generally appear; the left-right symmetric model is a  $SO(10)$  GUT extension of the SM, postulating the existence of a right-handed version of the weak interaction as well as an additional  $Z$  boson. Finally, the sequential standard model, where the couplings to quarks and leptons are as in the SM, may not be gauge invariant, but it serves as a good benchmark for comparisons of results.

In the search for  $Z'$  bosons, the latest results are from CDF analyzing dielectron resonances using  $819 \text{ pb}^{-1}$  of data. The invariant mass spectrum of dielectron events used in this search is shown in Fig. 41. No significant excess is seen at any mass value leading to a limit on the mass of a sequential, standard model-like  $Z'$  of  $m(Z') > 850 \text{ GeV}$  at 95% C.L. CDF also searches for pair production of doubly charged Higgs bosons in the lepton flavor violating modes  $H^{++} \rightarrow e^+\tau^+$  and  $H^{++} \rightarrow \mu^+\tau^+$  (and charge conjugates). At least three leptons are required in the final states so that the backgrounds are very small, and no events are observed in approximately  $350 \text{ pb}^{-1}$  of data. Interpreted in a left-right symmetric model, the corresponding mass limit on doubly charged Higgs bosons coupling to left-handed particles is  $m(H^{++}) > 114(112) \text{ GeV}$  at 95% C.L. in the  $e\tau$  ( $\mu\tau$ ) channel.

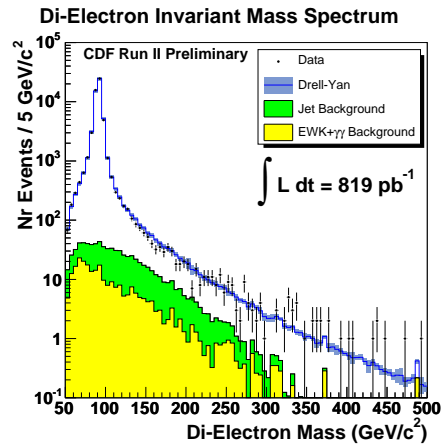


Figure 41: Dielectron invariant mass spectrum in the CDF search for electron-positron resonances.

In the search for singly charged gauge bosons, both  $D\mathcal{O}$  and CDF looked for a SM-like  $W'$  decaying to an

electron and a neutrino. The best limit, obtained from a study of the transverse mass spectrum in  $900 \text{ pb}^{-1}$  of data as shown in Fig. 42, is from  $D\bar{O}$  and requires  $m(W') > 965 \text{ GeV}$  at 95% C.L. (Fig. 43).

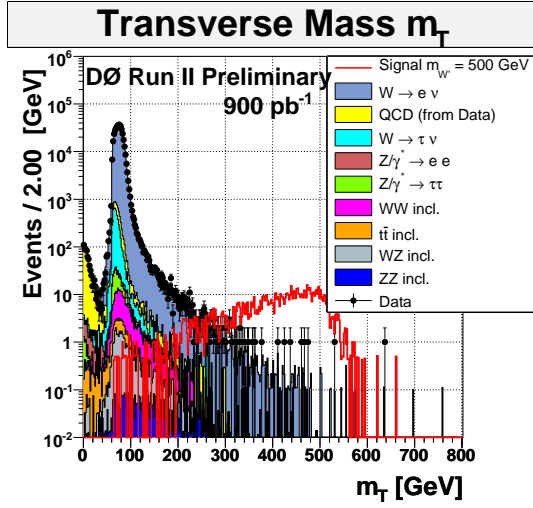


Figure 42: Transverse mass spectrum in the  $D\bar{O}$  search for  $W'$ . Also shown is the distribution for a hypothetical  $W'$  with a mass of 500 GeV.

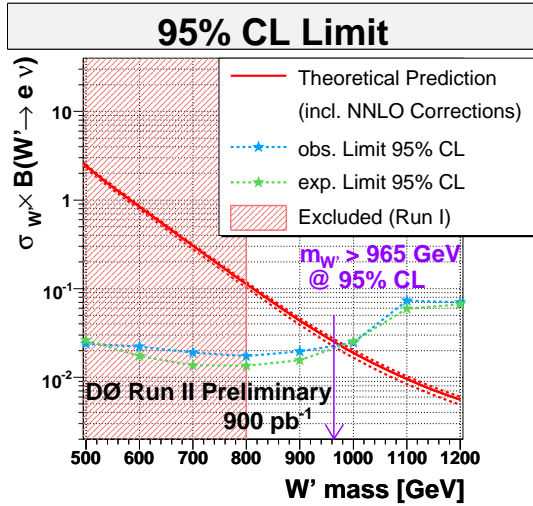


Figure 43: Cross section upper limits for the production of a SM-like  $W'$  obtained by  $D\bar{O}$ .

## 5. Leptoquarks

Leptoquarks are a natural consequence of the unification of quarks and leptons into a single multiplet, and as such are expected to be gauge bosons as well. While their masses may naturally be expected to be

of the order of the unification scale, in some models they can be relatively light. Experimentally, it is customary to consider one leptoquark per generation. These are assumed to be very short-lived and decay to a quark and a lepton. The branching fraction to a charged lepton and a quark is then denoted as  $\beta$ . At hadron colliders, leptoquarks can be pair-produced through the strong interaction, or are singly produced. In the latter case the production cross section depends on the (unknown) quark-lepton coupling, which is generally taken to be of the same order of magnitude as the fine structure constant.

Only the three most recent results from leptoquark searches at the Tevatron are discussed here.  $D\bar{O}$  has searched for scalar leptoquarks decaying to a quark and a neutrino ( $\beta = 0$ ) in the jets plus missing transverse energy topology in  $310 \text{ pb}^{-1}$  of data [27]. Experimentally this is a difficult analysis which suffers from substantial QCD dijet background due to mismeasured jets. To mitigate this,  $D\bar{O}$  requires exactly two acoplanar jets. The ensuing missing transverse energy distribution, before final analysis cuts, is shown in Fig. 44. The background from QCD dijet events, dominant at low missing transverse energy, is extrapolated to higher values using two different fitting functions as shown in the inset. The dominant non-QCD standard model background is  $Z$  boson plus jets production with the  $Z$  decaying to a pair of neutrinos. No excess is observed, so  $D\bar{O}$  sets a limit on the leptoquark mass of  $M_{LQ} > 136 \text{ GeV}$  at 95% C.L. (Fig. 45).

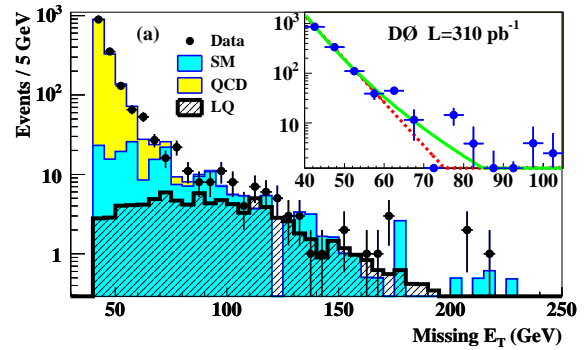


Figure 44: Missing transverse energy distribution in the  $D\bar{O}$  search for  $\beta = 0$  leptoquarks before final cuts. The inset shows the two different fitting functions used to evaluate the background from mismeasured QCD dijet events.

$D\bar{O}$  searched for the pair production of scalar third generation leptoquarks decaying into a tau neutrino and a  $b$  quark, leading to a final state of two  $b$  jets and  $\cancel{E}_T$ , identical to the sbottom search described earlier. Both jets are required to be identified as  $b$  jets using a lifetime based algorithm. Further cuts on  $\cancel{E}_T$  and  $H_T$  are optimized depending on the leptoquark mass  $M_{LQ}$ . For  $M_{LQ} = 220 \text{ GeV}$ ,  $\cancel{E}_T > 90 \text{ GeV}$  and  $H_T > 190 \text{ GeV}$ , one event is selected in the data cor-

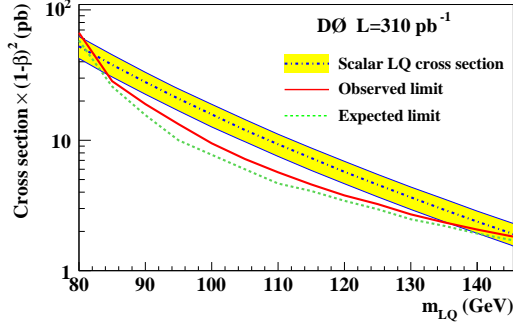


Figure 45: Cross section upper limits obtained in the search for  $\beta = 0$  scalar leptoquarks by  $D\bar{O}$ , together with the theoretical prediction.

responding to an integrated luminosity of  $310 \text{ pb}^{-1}$ , while  $2.6 \pm 0.6$  events are expected from SM backgrounds. In the absence of an excess in the data, a limit of  $M_{LQ} > 219 \text{ GeV}$  at 95% C.L. is set, assuming a branching fraction  $B(LQ \rightarrow b\nu) = 1$ ; allowing also decays to  $\tau t$ , the limit is reduced to  $M_{LQ} > 213 \text{ GeV}$  (Fig. 46).

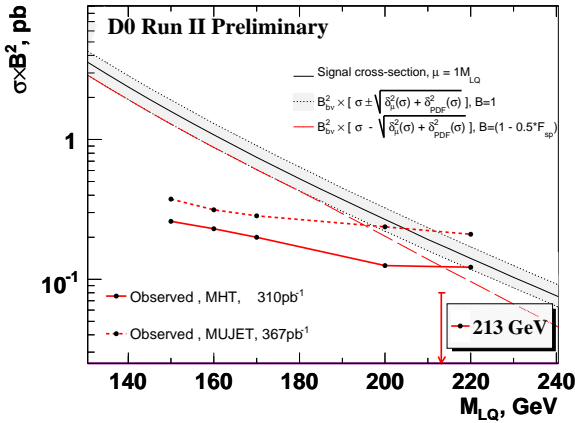


Figure 46: Cross section upper limits by  $D\bar{O}$  obtained in the search for  $\beta = 0$  scalar leptoquarks of the third generation, together with the theoretical prediction.

CDF has released results on a search for vector leptoquarks of the third generation in the  $LQ_3 \rightarrow b\tau$  decay channel. The signature consists of a dijet plus ditau final state, in which one tau is required to decay leptonically and the other hadronically. The main discriminating variables are the number of jets and an  $H_T$ -like variable, the scalar sum of the transverse energies of all jets, leptons and  $\cancel{E}_T$ . This allows CDF to set a limit at  $M_{LQ} > 294 \text{ GeV}$  assuming  $\beta = 1$  and using  $322 \text{ pb}^{-1}$  of data. Note that this limit is higher than the typical limits on leptoquark masses at the Tevatron due to the model choice of vector leptoquarks, which have a much larger production cross section than the scalar leptoquarks which are usually

chosen.

## 6. Large Extra Dimensions

Models postulating the existence of extra spatial dimensions have been proposed to solve the hierarchy problem posed by the large difference between the Planck scale  $M_{pl} \simeq 10^{16} \text{ TeV}$ , at which gravity is expected to become strong, and the scale of electroweak symmetry breaking,  $\simeq 1 \text{ TeV}$ . In the original large extra dimensions model of Arkani-Hamed, Dimopoulos and Dvali [28], in which only gravitons propagate in the bulk but all standard model fields are confined to a 3-brane, a tower of Kaluza-Klein excitations of the graviton emerges. The graviton states are too close in mass to be distinguished individually, and the coupling remains small, but the number of accessible states is very large. It is therefore possible to produce gravitons which immediately disappear into bulk space, leading to an excess of events with a high transverse energy jet and large missing transverse energy, the monojet signature:  $q\bar{q} \rightarrow gG$ ,  $qg \rightarrow qG$  and  $gg \rightarrow gG$ , where  $G$  is the emitted graviton. The dominant standard model backgrounds are the production of  $Z$  or  $W$  bosons plus jets, with the  $Z$  decaying to a pair of neutrinos or the lepton from the  $W$  decay escaping detection. Using  $1.1 \text{ fb}^{-1}$  of data, CDF has recently updated their published [29] analysis, and set limits on the effective Planck scale between  $M_D > 1.33 \text{ TeV}$  and  $M_D > 0.88 \text{ TeV}$  for a number of extra dimensions ranging from 2 to 6 (Fig. 47).

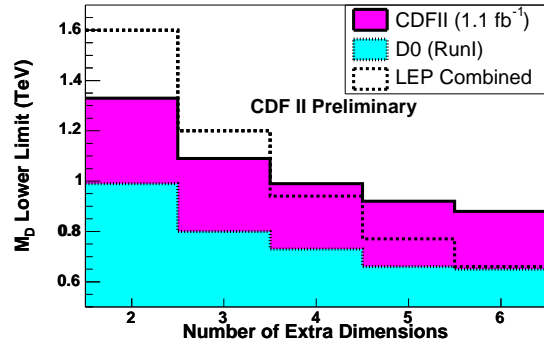


Figure 47: CDF limits on the effective Planck scale  $M_D$  as a function of the number of extra dimensions, compared to previous results.

In the model by Randall and Sundrum [30] gravity is located on a  $(3 + 1)$ -dimensional brane, the Planck brane, that is separated from the standard model brane in a fifth dimension with warped metric. In the simplest version of this model gravitons are the only particles that can propagate in the extra dimension. The gravitons appear as towers of Kaluza-Klein excitations with masses and widths determined by the parameters of the model. These parameters can

be expressed in terms of the mass of the first excited mode of the graviton,  $M_1$ , and the dimensionless coupling to the standard model fields,  $k\sqrt{8\pi}/M_{pl}$ . If it is light enough, the first excited graviton mode could be resonantly produced at the Tevatron. It is expected to decay to fermion-antifermion and to diboson pairs.

Both CDF and DØ have recently presented new results in the search for Randall-Sundrum gravitons based on  $0.8 - 1.2 \text{ fb}^{-1}$  (CDF) and  $1.1 \text{ fb}^{-1}$  (DØ) of data, respectively. Both experiments analyze the  $e^+e^-$  and  $\gamma\gamma$  final states. The invariant mass spectrum measured by DØ is shown in Fig. 48, and general agreement between data and the background expectation is observed. Using a sliding mass window, upper cross section limits are derived, which are then translated into lower mass limits for the lowest excited mode of Randall-Sundrum gravitons (Fig. 49). For a coupling parameter  $k\sqrt{8\pi}/M_{pl} = 0.1$  (0.01), masses  $M_1 < 865$  (240) GeV are excluded at the 95% C.L. by the DØ analysis. The corresponding CDF exclusion limits are  $M_1 < 875$  (242) GeV.

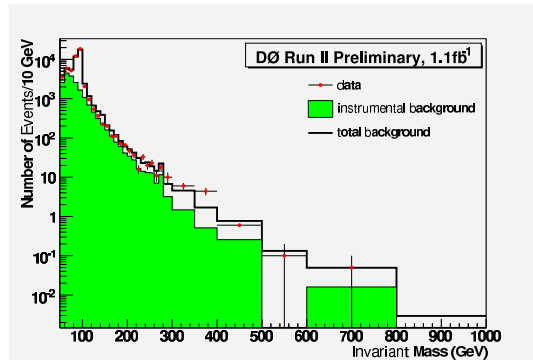


Figure 48: Invariant mass spectrum of diphotons and dielectrons observed by DØ in the search for Randall-Sundrum gravitons.

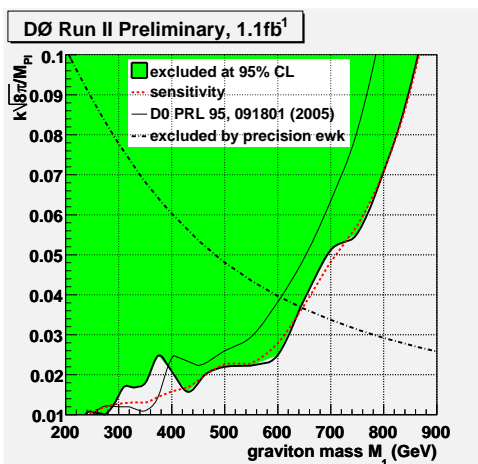


Figure 49: Excluded region in the plane of  $k\sqrt{8\pi}/M_{pl}$  and graviton mass by DØ.

## 7. Excited Fermions and Other Resonances

In the search for excited leptons, CDF has published previously [34] results of a search for excited electrons. Recently, both experiments have presented their analyses of excited muon production [35, 36]. They searched for associated production of a muon and an excited muon, with the latter decaying to a muon and a photon. The production is approximated as a contact interaction, while the decay is assumed to proceed either exclusively through a gauge interaction (CDF) or a combination of gauge and contact interactions, with the relative fraction of the two depending on the mass of the excited muon and the compositeness scale  $\Lambda$  (DØ). Both experiments obtain very similar results using  $371$  (CDF) and  $380$  (DØ)  $\text{pb}^{-1}$  of data. The DØ result is shown in Fig. 50, excluding for example  $m_{\mu^*} < 618$  GeV for  $\Lambda = 1$  TeV at 95% C.L. To make a comparison with LEP and HERA results easier, CDF also reinterprets the result in a gauge mediated model with Drell-Yan-like production of the  $\mu\mu^*$  pair with coupling  $f/\Lambda$ .

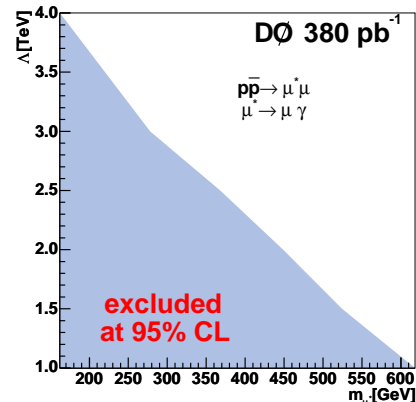


Figure 50: Exclusion region from the DØ search for excited muons produced in contact interactions in the decay mode  $\mu^* \rightarrow \mu\gamma$ .

Both CDF and DØ have presented recent results on the search for resonances decaying to dileptons +  $X$ . CDF has performed two analyses, with the first using  $H_T$  as its main discriminating variable. After selecting events with two high  $p_T$  leptons ( $e, \mu$ ), a control region with  $H_T < 200$  GeV is used to establish a good understanding of the data, and the signal region is chosen to have  $H_T > 400$  GeV, including at least two jets each with transverse energy  $E_T > 50$  GeV. Using  $929 \text{ pb}^{-1}$  of data, two events are observed in the signal region, with an expected background of  $2.9 \pm 1.5$  events. A limit of  $\sigma < 0.4 \text{ pb}$  at 90% C.L. is set on the production cross section of right-handed down-type quarks with a mass of 300 GeV as proposed in [31].

In a second analysis, CDF studied the transverse momentum distribution of  $Z$  bosons. This has the advantage of being insensitive to the nature of the other decay products, but it is of course more difficult and potentially less sensitive than a direct resonance search. Selecting events with a dielectron invariant mass compatible with the mass of the  $Z$  boson,  $66 < M_{ee} < 116$  GeV, CDF measured the  $Z$  transverse momentum distribution shown in Fig. 51. From this they determined an upper limit on the anomalous production of  $Z$  bosons as a function of transverse momentum using  $305 \text{ pb}^{-1}$  of data. The 95% C.L. limit ranges from about 1 pb for  $p_T(Z) = 20$  GeV to approximately 2 fb for  $p_T(Z) = 200$  GeV. A similar search was carried out in the  $Z \rightarrow \mu^+\mu^-$  channel.

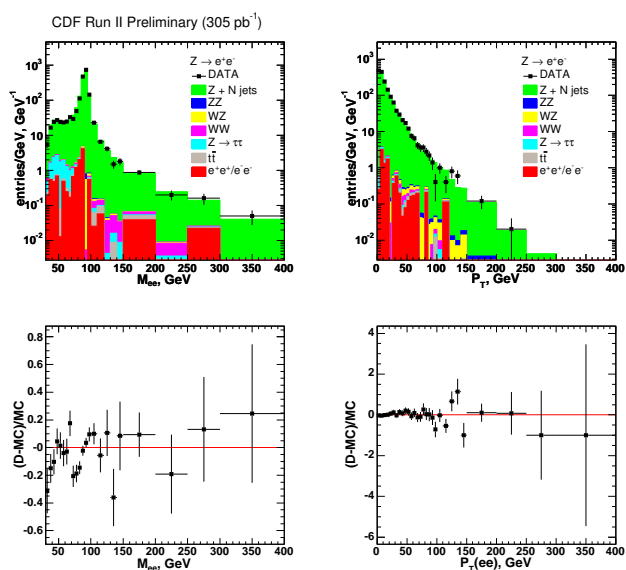


Figure 51: Invariant mass and transverse momentum distribution of electron-positron pairs measured by CDF in  $305 \text{ pb}^{-1}$  of data; a mass cut  $66 < M_{ee} < 116$  GeV has been applied for the right hand figures.

DØ explicitly searched for a  $Z$  boson plus jet resonance by combining the  $Z$  boson plus jet mass spectrum and the  $Z$  boson transverse momentum distribution as discriminating variables [32]. The invariant mass distribution, using the decay  $Z \rightarrow e^+e^-$  and events with  $80 < M_{ee} < 102$  GeV, measured in  $370 \text{ pb}^{-1}$  of data is shown in Fig. 52. No excess is observed and a limit is set on the mass of an excited quark as proposed in [33] at  $M_{q^*} > 520$  GeV at 95% C.L.

## 8. Events with Leptons and Photons

In Run I, CDF reported an excess of events with a photon, a lepton and large missing transverse energy compared to standard model expectations [37].

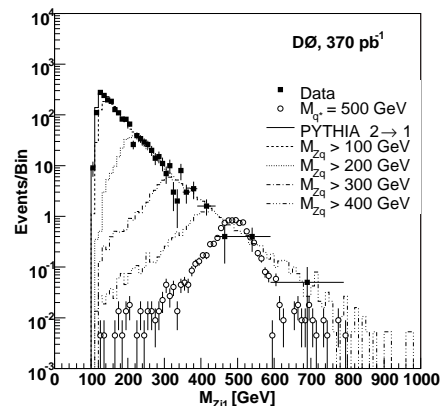


Figure 52: Invariant mass of the  $Z$  boson and leading jet as measured by DØ in  $370 \text{ pb}^{-1}$  of data. The curves with different  $M_{Zq}$  thresholds correspond to different generation thresholds for  $2 \rightarrow 2$  processes in Pythia, and the open circles represent the signal due to an excited quark of mass  $m_{q^*} = 500$  GeV and narrow width.

This excess, corresponding to a 2.7 sigma effect, was deemed “an interesting result”, but not “a compelling observation of new physics”. CDF has repeated this analysis in Run II using  $305 \text{ pb}^{-1}$  of data [38]. The data is now compatible with standard model expectations in all channels, suggesting that the excess observed in Run I was due to a statistical fluctuation.

In a similar spirit, CDF searches for events with two photons and an additional object, which can be an electron, a muon, a third photon, or  $\cancel{E}_T$ . The analysis is based on  $1.0 - 1.2 \text{ fb}^{-1}$  of data. In the  $\gamma\gamma + \cancel{E}_T$  search, a sliding cut on  $\cancel{E}_T$  from 20 to  $> 150$  GeV is used, and for all cut values agreement between the data and the background expectation is found. In the  $e\gamma\gamma$  and  $\mu\gamma\gamma$  final states, 1 and 0 events are selected in the data, while  $3.79 \pm 0.54$  and  $0.71 \pm 0.10$  events are expected from SM backgrounds. Finally, 4 events are found with three photons, with a background expectation of  $2.2 \pm 0.6$ . Unfortunately, no excess is observed over expectations.

## 9. Standard Model Higgs

The search for the SM Higgs is the focus of much attention both inside and outside the Tevatron community. Therefore its current state is briefly mentioned here.

The available results of SM Higgs searches at the Tevatron have recently been combined for the first time [39]. The results are for data corresponding to integrated luminosities ranging from  $360 - 1000 \text{ pb}^{-1}$  at CDF and  $260 - 950 \text{ pb}^{-1}$  at DØ. These searches are for SM Higgs bosons produced in association with vector bosons ( $p\bar{p} \rightarrow W/Z H \rightarrow l\nu b\bar{b}/\nu\bar{\nu} b\bar{b}/l^+l^- b\bar{b}$  or



$p\bar{p} \rightarrow WH \rightarrow WW^+W^-$ ) or singly through gluon-gluon fusion ( $p\bar{p} \rightarrow H \rightarrow W^+W^-$ ), separated into 16 mutually exclusive final states. Special care has been taken to account for systematic uncertainties and their correlations, and to ensure a statistically robust result. The combined result is shown in Fig. 53 in terms of the ratio of limits set to the SM cross sections as a function of Higgs mass. A value of  $< 1$  would indicate a Higgs mass excluded at 95% C.L. The observed limits are factors of 10.4 and 3.8 of the SM expectation at Higgs masses of  $m_H = 115$  GeV and  $m_H = 160$  GeV, respectively. These results represent an improvement in search sensitivity over those obtained for individual experiments, as can also be seen from Fig. 53. With the expected increase in integrated luminosity as well as improvements in analysis techniques, the Tevatron experiments have a realistic chance to reach sensitivity for a SM Higgs before the LHC delivers first results. Already now, the results are placing constraints on certain scenarios beyond the standard model, for example in models with four or more fermion generations [40] (Fig. 54).

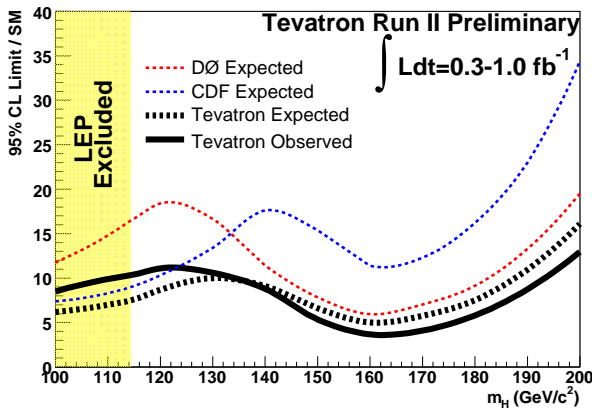


Figure 53: Expected and observed lower limits on the Higgs boson production cross section relative to the SM expectation, as a function of the Higgs mass. In addition to the combined result, the expected 95% C.L. ratios for the CDF and DØ experiments alone are shown.

## 10. Conclusions

Both the Tevatron and HERA continue their good performance, and the DØ, CDF, H1 and ZEUS experiments collect large amounts of data and search for new physics in many channels. Only recent results have been reported here, and many other analyses are in progress. From HERA, the most interesting results continue to be in the area of isolated leptons. At the Tevatron, many different models are tested with ever increasing sensitivity, but no discoveries are to be reported yet. So far, new physics has remained

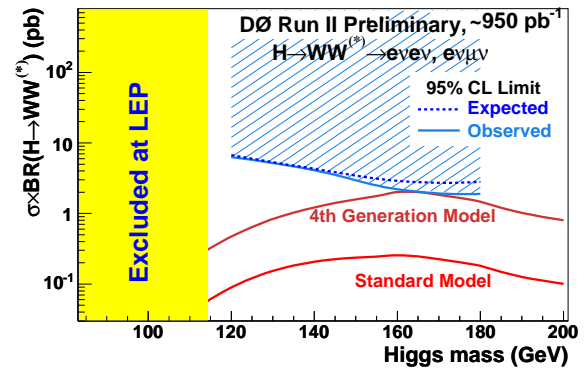


Figure 54: Excluded cross section times branching ratio at 95% C.L. in the DØ  $H \rightarrow W^+W^-$  analysis together with expectations from standard model Higgs boson production and an alternative model with four fermion generations.

hidden. The search for the SM Higgs continues with high priority, and a substantial amount of data is yet to be recorded and analyzed before the LHC can be expected to start delivering results.

## Acknowledgments

I would like to thank the organizers for a well organized conference with an exciting programme in a beautiful location. Many thanks to my colleagues from the DØ, CDF, H1 and ZEUS collaborations for their help in preparing this talk.

## References

- [1] B.W. Lee, C. Quigg and H.B. Thacker, Phys. Rev. D 16 (1977) 1519.
- [2] F. Englert and R. Brout, Phys. Rev. Lett. 13 (1964) 321; P.W. Higgs, Phys. Rev. Lett. 13 (1964) 508.
- [3] LEP Electroweak Working Group, <http://lepewwg.web.cern.ch/LEPEWWG/>.
- [4] Details for all Tevatron results can be found at <http://www-d0.fnal.gov/Run2Physics/WWW/results/np.htm>, <http://www-cdf.fnal.gov/physics/exotic/exotic.html>.
- [5] <http://www-h1.desy.de/h1det/lumi/>.
- [6] H1 Collaboration, *Observation of an  $e^+p \rightarrow \mu^+X$  Event with High Transverse Momenta at HERA*, DESY Report DESY 94-248 (1994).
- [7] H1 Collaboration, *Events with an Isolated Lepton and Missing Transverse Momentum at HERA*, <http://www-h1.desy.de/h1/www/publications/htmlsplit/H1prelim-06->

- 162.long.html, contributed paper to the ICHEP 2006 conference, update of Phys. Lett. B 561 (2003) 241 [hep-ex/0301030].
- [8] ZEUS Collaboration, *Search for Events with High- $p_T$  Isolated Leptons and Missing Transverse Momentum in  $e^\pm p$  Collisions at HERA I and HERA II*, contributed paper to the ICHEP 2006 conference, ZEUS preliminary result ZEUS-prel-06-012 and references therein; previous results in Phys. Lett. B 471 (2000) 411 [hep-ex/9907023].
- [9] H1 Collaboration, *Search for Events with Tau Leptons in  $ep$  Collisions at HERA*, <http://www-h1.desy.de/h1/www/publications/htmlsplit/H1prelim-06-064.long.html>, contributed paper to the ICHEP 2006 conference, update of hep-ex/0604022 (submitted to Eur. Phys. J. C).
- [10] ZEUS Collaboration, Phys. Lett. B 583 (2004) 41 [hep-ex/0311028].
- [11] ZEUS Collaboration, *Study of Multi-lepton Production with the ZEUS Detector at HERA*, contributed paper to the ICHEP 2006 conference, ZEUS preliminary result ZEUS-prel-06-017.
- [12] H1 Collaboration, *Multi-lepton Events at HERA*, <http://www-h1.desy.de/h1/www/publications/htmlsplit/H1prelim-06-063.long.html>, contributed paper to the ICHEP 2006 conference, update of Eur. Phys. J. C 31 (2003) 17 [hep-ex/0307015] and Phys. Lett. B 583 (2004) 28 [hep-ex/0311015].
- [13] H1 Collaboration, *Generic Analysis on HERA II Data*, <http://www-h1.desy.de/h1/www/publications/htmlsplit/H1prelim-06-161.long.html>, contributed paper to the ICHEP 2006 conference; HERA I data: Phys. Lett. B 602 (2004) 14 [hep-ex/0408044].
- [14] DØ Collaboration, Phys. Lett. B 638 (2006) 119 [hep-ex/0604029].
- [15] DØ Collaboration, *Search for Pair Production of Scalar Bottom Quarks in  $p\bar{p}$  Collisions at  $\sqrt{s} = 1.96$  TeV*, accepted by Phys. Rev. Lett. [hep-ex/0608013].
- [16] N. Arkani-Hamed, S. Dimopoulos, G.F. Giudice and A. Romanino, Nucl. Phys. B 709 (2005) 3 [hep-ph/0409232].
- [17] S. Weinberg, Phys. Rev. D 26 (1982) 287; N. Sakai and T. Yanagida, Nucl. Phys. B 197 (1982) 533.
- [18] B. C. Allanach, A. Dedes and H.K. Dreiner, Phys. Rev. D 60, 075014 (1999) [hep-ph/9906209].
- [19] R. Barbier *et al.*, Phys. Rep. 420 (2005) 1 [hep-ph/0406039].
- [20] DØ Collaboration, Phys. Lett. B 638 (2006) 441 [hep-ex/0605005].
- [21] DØ Collaboration, *Search for Neutral Long-Lived Particles Decaying into Two Muons in  $p\bar{p}$  Collisions at  $\sqrt{s} = 1.96$  TeV*, accepted by Phys. Rev. Lett. [hep-ex/0607028].
- [22] NuTeV Collaboration, Phys. Rev. Lett. 87 (2001) 041801 [hep-ex/0104037].
- [23] DØ Collaboration, Phys. Rev. Lett. 97 (2006) 111801 [hep-ex/0605010].
- [24] CDF Collaboration, Phys. Rev. Lett. 96 (2006) 011802 [hep-ex/0508051].
- [25] DØ Collaboration, Phys. Rev. Lett. 95 (2005) 151801 [hep-ex/0504018]; DØ Collaboration, *Search for Neutral Higgs Bosons Decaying to Tau Pairs in  $p\bar{p}$  Collisions at  $\sqrt{s} = 1.96$  TeV*, accepted by Phys. Rev. Lett. [hep-ex/0605009].
- [26] M. Carena, S. Heinemeyer, C.E.M. Wagner and G. Weiglein, Eur. Phys. J. C 45 (2006) 797 [hep-ph/0511023].
- [27] DØ Collaboration, Phys. Lett. B 640 (2006) 230 [hep-ex/0607009].
- [28] N. Arkani-Hamed, S. Dimopoulos and G.R. Dvali, Phys. Lett. B 429 (1998) 263 [hep-ph/9803315].
- [29] CDF Collaboration, *Search for Large Extra Dimensions in the Production of Jets and Missing Transverse Energy in  $p\bar{p}$  Collisions at  $\sqrt{s} = 1.96$  TeV*, submitted to Phys. Rev. Lett. [hep-ex/0605101].
- [30] L. Randall and R. Sundrum, Phys. Rev. Lett. 83 (1999) 3370 [hep-ph/9905221] and 4690 [hep-th/9906064].
- [31] J.D. Bjorken, S. Pakvasa and S.F. Tuan, Phys. Rev. D 66 (2002) 053008 [hep-ph/0206116].
- [32] DØ Collaboration, Phys. Rev. D 74 (2006) 011104 [hep-ex/0606018].
- [33] U. Baur, M. Spira and P.M. Zerwas, Phys. Rev. D 42 (1990) 815.
- [34] CDF Collaboration, Phys. Rev. Lett. 94 (2005) 101802 [hep-ex/0410013].
- [35] DØ Collaboration, Phys. Rev. D 73 (2006) 111102 [hep-ex/0604040].
- [36] CDF Collaboration, *Search for Excited and Exotic Muons in the  $\mu\gamma$  Decay Channel in  $p\bar{p}$  Collisions at  $\sqrt{s} = 1.96$  TeV*, submitted to Phys. Rev. Lett. [hep-ex/0606043].
- [37] CDF Collaboration, Phys. Rev. Lett. 89 (2002) 041802 [hep-ex/0202044].
- [38] CDF Collaboration, Phys. Rev. Lett. 97 (2006) 031801 [hep-ex/0605097].
- [39] TEVNPH Working Group, *Combined DØ and CDF Upper Limits on Standard Model Higgs Boson Production*, CDF Note 8384 and DØ Note 5227 (2006) and references therein, [http://tevnpwg.fnal.gov/results/d0conf\\_5227/d0conf\\_5227.pdf](http://tevnpwg.fnal.gov/results/d0conf_5227/d0conf_5227.pdf).
- [40] E. Arik, O. Çakir, S.A. Çetin and S. Sultansoy, *Observability of the Higgs Boson and Extra SM Families at the Tevatron* [hep-ph/0502050]; E. Arik, M. Arik, S.A. Çetin, T. Çonka, A. Mailov and S. Sultansoy, Eur. Phys. J. C 26 (2002) 9 [hep-ph/0109037].